Low luminosity Type II supernovae – II. Pointing towards moderate mass precursors

S. Spiro,[1][*] A. Pastorello,[1] M. L. Pumo,[1,2] L. Zampieri,[1] M. Turatto,[1] S. J. Smartt,[3]
S. Benetti,[1] E. Cappellaro,[1] S. Valenti,[4,5] I. Agnoletto,[1] G. Altavilla,[6] T. Aoki,[7]
E. Brocato,[8] E. M. Corsini,[1,9] A. Di Cianno,[10] N. Elias-Rosa,[11] M. Hamuy,[12]
K. Enya,[13] M. Fiaschi,[9] G. Folatelli,[14] S. Desidera,[1] A. Harutyunyan,[15]
D. A. Howell,[4,5] A. Kawka,[16] Y. Kobayashi,[17] B. Leibundgut,[18] T. Minezaki,[7]
H. Navasardyan,[1] K. Nomoto,[19,20] S. Mattila,[21] A. Pietrinferni,[10] G. Pignata,[22]
G. Raimondo,[10] M. Salvo,[23] B. P. Schmidt,[23] J. Sollerman,[24] J. Spyromilio,[18]
S. Taubenberger,[25] G. Valentini,[10] S. Vennes[16] and Y. Yoshii[7]

[1]*INAF–Astronomical Observatory of Padua, Vicolo dell'Osservatorio 5, I-35122 Padua, Italy*
[2]*INAF–Astrophysical Observatory of Catania, via S. Sofia 78, I-95123 Catania, Italy*
[3]*Astrophysics Research Centre, School of mathematics and Physics, Queen's University Belfast, Belfast BT7 INN, UK*
[4]*Las Cumbres Observatory Global Telescope Network, 6740 Cortona Dr, Suite 102, Goleta, CA 93117, USA*
[5]*Department of Physics, University of California, Santa Barbara, Broida Hall, Mail Code 9530, Santa Barbara, CA 93106-9530, USA*
[6]*Osservatorio Astronomico di Bologna, INAF, Via C. Ranzani, 1, I-40127 Bologna, Italy*
[7]*Kiso Observatory, Institute of Astronomy, School of Science, The University of Tokyo, 10762-30 Mitake, Kiso, Nagano 397-0101, Japan*
[8]*INAF–Osservatorio Astronomico di Roma, Via Frascati 33, I-00040 Monte Porzio Catone, Italy*
[9]*Dipartimento di Fisica e Astronomia 'G. Galilei', Universitá di Padova, vicolo dell'Osservatorio 3, I-35122 Padova, Italy*
[10]*INAF–Osservatorio Astronomico di Teramo, via M. Maggini, I-64100 Teramo, Italy*
[11]*Institut de Ciències de l'Espai (IEEC-CSIC), Facultat de Ciències, Campus UAB, E-08193 Bellaterra, Spain*
[12]*Departamento de Astronoma, Universidad de Chile, Casilla 36-D, Santiago, Chile*
[13]*Institute of Space and Astronautical Science, Japan Aerospace Exploration Agency, 3-1-1, Yoshinodai, Sagamihara, Kanagawa 229-8510, Japan*
[14]*Kavli Institute for the Physics and Mathematics of the Universe (WPI), Todai Institutes for Advanced Study, the University of Tokyo (Kavli IPMU, WPI), Kashiwa 277-8583, Japan*
[15]*Fundacion Galileo Galilei–INAF, Telescopio Nazionale Galileo, E-38700 Santa Cruz de la Palma, Tenerife, Spain*
[16]*Astronomický ústav, AV CŘ, Fričova 298, CZ-251 65 Ondřejov, Czech Republic*
[17]*National Astronomical Observatory, 2-21-1 Osawa, Miaka, Tokyo 181-8588, Japan*
[18]*ESO, Karl-Schwarzschild-Strasse 2, D-85748 Garching, Germany*
[19]*Kavli Institute for the Physics and Mathematics of the Universe (WPI), The University of Tokyo, 5-1-5 Kashiwanoha, Kashiwa, Chiba 277-8583, Japan*
[20]*Department of Astronomy, School of Science, The University of Tokyo, 7-3-1 Hongo, Bunkyo-ku, Tokyo 113-0033, Japan*
[21]*Finnish Centre for Astronomy with ESO (FINCA), University of Turku, Väisäläntie 20, FI-21500 Piikkiö, Finland*
[22]*Departamento de Ciencias Fisicas, Universidad Andres Bello, Avda. Republica 252, Santiago, Chile*
[23]*Research School of Astronomy and Astrophysics, Australian National University, Cotter Road, Weston Creek, PO 2611, Australia*
[24]*Oskar Klein Centre, Department of Astronomy, AlbaNova, Stockholm University, SE-10691 Stockholm, Sweden*
[25]*Max-Planck-Institut für Astrophysik, Karl-Schwarzschild-Str. 1, D-85741 Garching bei München, Germany*

ABSTRACT

We present new data for five underluminous Type II-plateau supernovae (SNe IIP), namely SN 1999gn, SN 2002gd, SN 2003Z, SN 2004eg and SN 2006ov. This new sample of low-luminosity SNe IIP (LL SNe IIP) is analysed together with similar objects studied in the past. All of them show a flat light-curve plateau lasting about 100 d, an underluminous late-time exponential tail, intrinsic colours that are unusually red, and spectra showing prominent and narrow P Cygni lines. A velocity of the ejected material below 10^3 km s^{-1} is inferred from measurements at the end of the plateau. The ^{56}Ni masses ejected in the explosion are very

[*] E-mail: susanna.spiro@oapd.inaf.it

small ($\leq 10^{-2}$ M$_\odot$). We investigate the correlations among ^{56}Ni mass, expansion velocity of the ejecta and absolute magnitude in the middle of the plateau, confirming the main findings of Hamuy, according to which events showing brighter plateau and larger expansion velocities are expected to produce more ^{56}Ni. We propose that these faint objects represent the LL tail of a continuous distribution in parameters space of SNe IIP. The physical properties of the progenitors at the explosion are estimated through the hydrodynamical modelling of the observables for two representative events of this class, namely SN 2005cs and SN 2008in. We find that the majority of LL SNe IIP, and quite possibly all, originate in the core collapse of intermediate-mass stars, in the mass range 10–15 M$_\odot$.

Key words: supernovae: general – supernovae: individual: SN 1999gn – supernovae: individual: SN 2002gd – supernovae: individual: SN 2003Z – supernovae: individual: SN 2004eg – supernovae: individual: SN 2006ov.

1 INTRODUCTION

In recent years, a number of underluminous transient events observed in nearby galaxies, with peculiar observed properties have provoked interest in their physical origins and explosion mechanisms. They lie in the gap of the absolute magnitude versus photometric evolutionary time-scales diagram ($-10 > M_R > -14$ mag; see Kulkarni et al. 2007; Rau et al. 2009) separating the brightest novae and the faintest known supernovae (SNe). These new discoveries include a number of faint, ^{56}Ni-poor, low expansion velocity hydrogen free SNe (e.g. SN 2008ha; Valenti et al. 2009; Foley et al. 2009), some ultrafaint objects with Type IIn SN-like spectra and shape of the light curves resembling those of Type IIL or Type IIP SNe (NGC300 OT2008-1, Berger et al. 2009; Bond et al. 2009, SN 2008S, Botticella et al. 2009; Smith et al. 2009, M85 OT2006-1, Kulkarni et al. 2007; Pastorello et al. 2007), and even a subluminous SN 1987A-like event (SN 2009E, Pastorello et al. 2012).

Whilst the nature of many of these objects is still far from being unveiled (unusual eruptive events or real SNe, partial deflagrations or low-energy genuine SNe, electron-capture SNe from moderate-mass stars or fall-back core-collapse (CC) SNe from massive progenitors), major progresses have been made during the past decade for a specific class of underluminous transients: the faint SNe IIP (Pastorello et al. 2004, which is Paper I in this series).

The prototype of this class is SN 1997D. It was discovered on January 14.15 UT in NGC 1536 (de Mello, Benetti & Massone 1997) and it was at that time the faintest and the most subenergetic Type II SN ever discovered. The comparison of the light curve with those of other Type II SNe, suggested the ejection of very low amount of ^{56}Ni (Turatto et al. 1998; Benetti et al. 2001). Unfortunately SN 1997D was discovered when it was quite old, so the explosion epoch was not well constrained. It had unusually red spectra suggesting low continuum temperatures, and narrow spectral lines indicative of slow-moving ejecta (1000 km s^{-1}, that is 3–4 times lower than in normal SN IIP explosions). All of this suggested a rather low explosion energy for SN 1997D (of the order of 10^{-1} foe).

In past years, two alternative scenarios have been proposed to explain SN 1997D. The first invokes a low-energy explosion of a high-mass (more than 25 M$_\odot$) star (Turatto et al. 1998) in which a large amount of stellar material remains bound to the core after the collapse, and falls back on to it, increasing its mass (Zampieri, Shapiro & Colpi 1998). In this case the compact remnant may be either a black hole or a neutron star. The crucial parameter to discriminate between the two types of remnants is indeed the amount of stellar material falling back on to the core. An alternative scenario was proposed by Chugai & Utrobin (2000), in which the precursor star of moderate mass ($\sim$8–11 M$_\odot$) develops a degenerate NeO core (see e.g. Pumo 2007; Pumo et al. 2009, and references therein for a discussion on the evolution of this stellar type) and undergoes a CC triggered by electron capture (Nomoto 1984; Takahashi, Yoshida & Umeda 2013). In this case the fall back is negligible and the explosion leaves behind a neutron star.

As mentioned above, the explosion epoch of SN 1997D was poorly constrained. Several models assumed a plateau duration of about 40–60 d (e.g. Chugai & Utrobin 2000), while others a more conventional length of about 100 d (e.g. Zampieri et al. 2003).

Subsequent discoveries of a number of SN 1997D-like events established that most of them had long-lasting plateau ($\sim$100 d), implying that the results obtained from the preliminary modelling to the data of SN 1997D needed to be revised. Several objects were indeed discovered very close to the explosion epoch and proved that their plateaus were significantly longer than thought before (e.g. SNe 1999br, 2001dc and 2003Z, Pastorello et al. 2004). These new observations allowed a consistent calibration of the explosion dates also for events discovered at later phases, such as SN 1997D, and hence their explosion and ejecta parameters were better constrained.

With more complete data sets and/or recalibrated explosion epochs, the masses inferred from hydrodynamic models were initially estimated to be relatively high. Zampieri et al. (2003) found a progenitor of about 16 M$_\odot$ for SN 1999br and 19 M$_\odot$ for SN 1997D. Similar results were obtained by Utrobin, Chugai & Pastorello (2007) with a mass in the range 14.4–17.4 M$_\odot$ for the progenitor of SN 2003Z, while Utrobin & Chugai (2008) and Pastorello et al. (2009) estimated the red supergiant precursor of SN 2005cs to be 18.2 ± 1.0 and 10–15 M$_\odot$, respectively. Therefore, based on SN data modelling, the masses of low-luminosity (LL) SNe IIP progenitor were estimated in the range 10–19 M$_\odot$.

An independent estimate of the masses of the SN progenitor is based on the direct detection of the precursor star in archive images obtained before the SN explosion (Van Dyk, Li & Filippenko 2003; Smartt et al. 2004, 2009; Smartt 2009, and reference therein). The detection of a progenitor (or the measurement of deep upper magnitude limits) on images obtained with different filters allows us to estimate the absolute luminosity and the colours (and, from these, the temperature) of the putative progenitor star. Hence, from matching theoretical evolutionary tracks, it is possible to estimate its mass. In the last decade a handful of LL SNe IIP have been studied with this method: SN 2005cs (Maund, Smartt & Danziger 2005; Li et al. 2006; Eldridge, Mattila & Smartt 2007; Maund, Reilly &

Mattila 2014), SN 2008bk (Mattila et al. 2008; Van Dyk et al. 2012; Maund et al. 2014; Pignata et al., in preparation) and SN 2009md (Fraser et al. 2011) for which lower mass progenitors of 8–13 $M_\odot$ were inferred. For two additional LL SNe IIP, SN 1999br (Maund & Smartt 2005; Smartt et al. 2009) and SN 2006ov (Crockett et al. 2011), progenitor mass limits of $M < 15\ M_\odot$ and $M < 10\ M_\odot$, respectively, were estimated.

Currently, the masses of precursors of LL SNe IIP are still uncertain, with conflicting results obtained through hydrodynamic modelling of SN data, which indicates a distribution extending to rather massive progenitors (∼10–20 $M_\odot$) or from the direct detection of progenitors in pre-SN images, which suggests lower mass (∼8–13 $M_\odot$) stars. The problem of this discrepancy has been raised by Utrobin & Chugai (2009), that tentatively attributed an overestimate of the ejecta masses to the one-dimensional approximation of the hydrodynamical models. Dessart et al. (2013) suggested it may be related to the pre-SN structure being not well understood.

On the other hand it is fair to say that estimate from the direct detection of the progenitor presents a number of caveats. First of all this method can be applied only to nearby objects within a small volume, e.g. those that explode within ∼30 Mpc. Uncertainties in the stellar evolutionary models used to infer the progenitor mass (e.g. treatment of overshooting and mass-loss) can also lead to different inferred masses, although none of the codes available differ by large factors (Smartt et al. 2009). Finally reliable extinction estimates are essential and there is a risk of underestimating the mass of the progenitor (Walmswell & Eldridge 2012). Kochanek, Khan & Dai (2012) also note that the extinction by circumstellar dust may be significantly different from that of interstellar dust and that the effect of circumstellar (CSM) dust may not raise progenitor estimates as significantly as proposed by Walmswell & Eldridge (2012). Systematic studies of a larger number of well-followed faint SNe IIP will allow us to improve our knowledge of these events and, in particular, of the parameters describing the progenitor star and its explosion (including ^{56}Ni mass, total ejected mass, initial radius, kinetic energy).

In this paper we present new data (both photometry and spectroscopy) for five subluminous SNe classified as LL SNe IIP: SN 2002gd, SN 2003Z, SN 2004eg, SN 1999gn and SN 2006ov. These SNe, in analogy with SN 1997D, are intrinsically faint compared with more canonical SNe IIP (the typical luminosity in the plateau phase for a normal Type IIP is $L \sim 10^{42}$–10^{43} erg s^{-1}). Together with other LL SNe IIP presented in previous works i.e. SN 1994N, SN 1997D, SN 1999br, SN 1999eu, SN 2001dc, SN 2005cs (Turatto et al. 1998; Benetti et al. 2001; Pastorello et al. 2004, 2006, 2009) and other events recently published, i.e. SN 2008bk (Van Dyk et al. 2012; Pignata et al., in preparation), SN 2008in (Roy et al. 2011), SN 2009N (Takáts et al. 2014), SN 2009md (Fraser et al. 2011) and SN 2010id (Gal-Yam et al. 2011), we collect an extensive sample of LL SNe IIP. As the best observed underluminous SN IIP, SN 2005cs (Pastorello et al. 2006, 2009; Tsvetkov et al. 2006; Brown et al. 2007; Dessart et al. 2008) can be considered as a template for this SN family. In particular, the multiwavelength study of SN 2005cs is useful to derive the bolometric light curves of all other LL SNe IIP (with caveats described in the text). In addition, the properties of its red supergiant progenitor star were extensively discussed (Maund et al. 2005; Li et al. 2006; Takáts & Vinkó 2006; Eldridge et al. 2007; Dessart et al. 2008; Utrobin & Chugai 2008), and – likely – well constrained. These results will be compared with our findings for other LL SNe IIP.

This paper is organized as follows: in Section 2 we present the new LL SN IIP sample and introduce the properties of the host
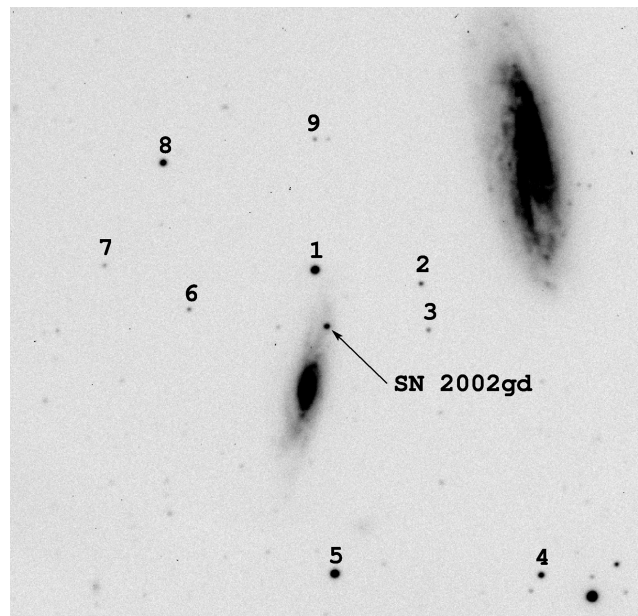

Figure 1. SN 2002gd and the local sequence stars (TNG + Dolores, *R*-band image obtained on 2002 December 28, with an exposure time of 3 min). East is up, north is to the right.

galaxies. In Section 3 we give a summary of the observations with a brief description of the instruments used. Photometric data are presented in Section 4, including light curves (Section 4.1), colour curves (Section 4.2) and bolometric light curves (Section 4.3). Spectroscopic data are shown in Section 5: properties of individual objects are illustrated in Section 5.1, while the common properties for the entire group are discussed in Section 5.2. Estimates of the physical parameters of our SN sample and a discussion on the implications for the nature of the progenitor stars are in Sections 6 and 7, respectively. Finally a summary follows in Section 8.

2 THE NEW SAMPLE: SUPERNOVAE AND HOST GALAXIES

We present here relevant data for the new LL SNe sample and their host galaxies. Except in the case of SN1999gn and SN 2006ov (see Section 2.4) for which a Tully–Fisher distance is adopted, in all other cases the SN distances are estimated using the recessional velocity corrected for Local Group infall into the Virgo Cluster (v_{Vir} parameter from the HYPERLEDA data base,[1] Paturel et al. 2003) assuming an Hubble constant H$_0$ = 72 km s^{-1} Mpc^{-1}.

No evidence of extinction within the host galaxies were found, therefore we consider only the Galactic contribution estimated by Schlafly & Finkbeiner (2011).

2.1 SN 2002gd

SN 2002gd (Fig. 1) was independently discovered by Klotz et al. (2002). The earliest detection was recorded on 2002 October 5.31 UT at an unfiltered CCD magnitude of 18.9 (Klotz & Jasinski 2002). Nothing was visible at the position of the SN on September 15.95 UT (Klotz & Jasinski 2002), indicating that the SN was

---

[1] http://leda.univ-lyon1.fr/

Table 1. Main observational data of SN 1999gn, SN 2006ov, SN 2002gd, SN 2003Z, SN 2004eg and their host galaxies. $m_V^{\rm pl}$ is the mean plateau magnitude in the V band.

SN Data	2002gd		2003Z		2004eg		1999gn		2006ov	
α (J2000.0)	$23^{\rm h}14^{\rm m}36\!\!\overset{\rm s}{.}98$	§	$09^{\rm h}07^{\rm m}32\!\!\overset{\rm s}{.}46$	♠	$04^{\rm h}28^{\rm m}08\!\!\overset{\rm s}{.}26$	◇	$12^{\rm h}21^{\rm m}57\!\!\overset{\rm s}{.}02$	♣	$12^{\rm h}21^{\rm m}55\!\!\overset{\rm s}{.}30$	⊖
δ (J2000.0)	$+04°30'05\!\!''.7$	§	$+60°29'17\!\!''.5$	♠	$+21°39'18\!\!''.3$	◇	$+04°27'45\!\!''.6$	♣	$+04°29'16\!\!''.7$	⊖
Offset SN-Gal.Nucleus	$36''.8$E, $10''.8$N	§	$8''.4$W, $31''.0$N	♠	$20''$W, $1''.4$S	◇	$31''.7$E, $39''.8$S	♣	$5''.5$E, $51''$N	⊖
Discovery date (UT)	2002 Oct 5.31	§	2003 Jan 29.7	♠	2004 Sept 1.488	◇	1999 Dec 17.22	♣	2006 Nov 24.86	⊖
Discovery Julian Date	2452552.81	§	2452669.2	♠	2453249.5	◇	2451529.7	♣	2454064	⊖
Adopted explosion epoch (JD)	2452552	×	2452665	×	2453170	×	2451520	×	2453974	×
Discovery magnitude	$m = 18.9$	§	$m = 16.7$	♠	$m = 19.5$	◇	$m = 16.0$	♣	$m = 14.9$	⊖
$m_V^{\rm pl}$	17.56	×	17.53	×	19.16	×	-	×	15.73	×
Total extinction $A_{B,{\rm tot}}$	0.243	×	0.141	×	1.635	×	0.081	×	0.081	×
Host galaxies data	NGC 7537		NGC 2742		UGC 3053		NGC 4303			
α (J2000.0)	$23^{\rm h}14^{\rm m}34\!\!\overset{\rm s}{.}50$	†	$09^{\rm h}07^{\rm m}33\!\!\overset{\rm s}{.}53$	†	$04^{\rm h}28^{\rm m}09\!\!\overset{\rm s}{.}6$	†	$12^{\rm h}21^{\rm m}54\!\!\overset{\rm s}{.}9$	†		
δ (J2000.0)	$+04°29'54\!\!''.1$	†	$\delta +60°28'45\!\!''.6$	†	$+21°39'19\!\!''.0$	†	$+04°28'25\!\!''.0$	†		
Morph. type	SAbc:	†	SA(s)c:	†	Scd:	†	SAB(rs)bc	†		
B magnitude	13.86	†	12.03	†	14.75	†	10.18	†		
Galactic extinction A_B	0.243	⊗	0.141	⊗	1.635	⊗	0.081⊗			
Diameters	2.2 arcmin × 0.6 arcmin	†	3.0 arcmin × 1.5 arcmin	†	0.9 arcmin × 0.7 arcmin	†	6.5 arcmin × 5.8 arcmin	†		
$v_{\rm Vir}$ (km s^{-1})	2698	★	1511	★	2434	★	1616	†		
μ ($H_0 = 72$ km s^{-1} Mpc^{-1})	32.87	×	31.7	×	32.64	×	30.5	×		

♣ Dimai & Li (1999); × this paper; ⊖ Nakano et al. (2006); † NED; ⊗ Schlafly & Finkbeiner (2011); ★ HYPERLEDA; § Klotz & Jasinski (2002); ♠ Boles et al. (2003); ◇ Young et al. (2004).

caught very young, during the steep rise to the maximum light. Puckett provided the position of the SN at $\alpha = 23^{\rm h}14^{\rm m}36\!\!\overset{\rm s}{.}98$ and $\delta = +04°30'05\!\!''.7$ (equinox 2000.0), that was $36''.8$ east and $10''.8$ north of the nucleus of the galaxy NGC 7537. The SN was spectroscopically classified as a young SN II with a very blue continuum and H Balmer and He I 5876 Å lines showing low-contrast P Cygni profiles. The position of the blueshifted minima provide an expansion velocity $v \sim 5000$ km s^{-1} (Hamuy 2002), which is relatively low for such an early epoch (Benetti et al. 2002; Filippenko & Chornock 2002). From the characteristics of the early time spectra and light-curve evolution, we can constrain the explosion epoch with a small uncertainty to be 2002 October 4, i.e. JD = 245 2552 ± 2.

The host galaxy of SN 2002gd and NGC 7537, is of Sbc type. Relevant data for SN 2002gd and the host galaxy are reported in Table 1.

2.2 SN 2003Z

SN 2003Z (Fig. 2) was discovered by Qiu & Hu (Boles et al. 2003) with the Beijing Astronomical Observatory (BAO) 0.6-m telescope on 2003 January 29.7, when the SN magnitude was ~ 16.7, and confirmed with Katzman Automatic Imaging Telescope (KAIT) on 2003 January 30.4 (magnitude 16.5). It was located at $\alpha = 09^{\rm h}07^{\rm m}32\!\!\overset{\rm s}{.}46$ and $\delta = +60°29'17\!\!''.5$ (equinox 2000.0), close to an arm of NGC 2742 (8.4 arcsec west and 31.0 arcsec north of the nucleus of the host galaxy). Another BAO image obtained on 2003 January 20.7 showed nothing at the SN position, suggesting that SN 2003Z was discovered shortly after the explosion (JD = 245 2665 ± 4.5). Matheson et al. (2003) obtained a spectrum on 2003 January 31.36 showing a very blue continuum with well-defined P Cygni lines of H and He I. The estimated expansion velocity as derived from the minimum of Hβ was 6800 km s^{-1} (Matheson et al. 2003), again rather low in comparison with the velocity of canonical SNe IIP a few days after the explosion.

NGC 2742 belongs to the small group of galaxies LGG 167 (Garcia 1993) that has a mean radial velocity of 1475 km s^{-1}. The peculiar velocity of NGC 2742 inside the group is +66 km s^{-1}.
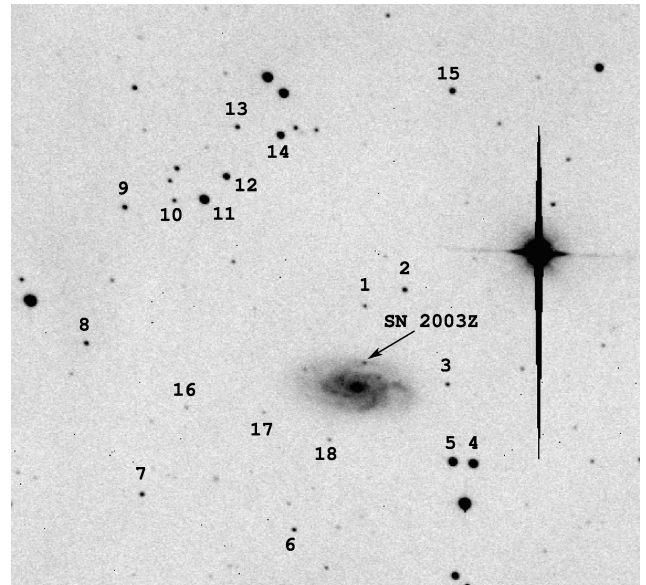

Figure 2. SN 2003Z in NGC 2742 and the local sequence stars [R-band image obtained on 2003 May 21 with the Newton 0.4 m telescope of the *Gruppo Astrofili di Padova* (Italy)]. North is up, east is to the left.

The correction for peculiar motion was taken into account in the distance modulus estimation.

Information on SN 2003Z and its host galaxy is in Table 1.

2.3 SN 2004eg

SN 2004eg (Fig. 3) was first detected in UGC 3053 by Young using the Table Mountain observatory 0.60-m reflector on 2004 September 1.488 UT (Young, Boles & Li 2004). The SN was located at $\alpha = 04^{\rm h}28^{\rm m}08\!\!\overset{\rm s}{.}26$, $\delta = +21°39'18\!\!''.3$ (equinox 2000.0), 20 arcsec west and 1.4 arcsec south of the nucleus of UGC 3053. The SN was not present on the Sky Survey images dating 1988–1991 (limiting red mag 20.8–21.5; limiting blue mag 21.5–22.5) and it was classified as a Type II SN by Filippenko et al. (2004). The line
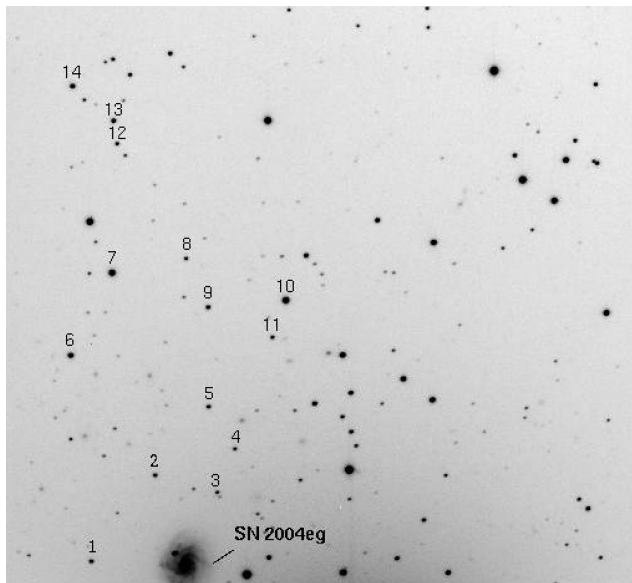
Figure 3. Position of SN 2004eg in UGC 3053 and local sequence stars [*V* band image obtained on 2004 December 1 with the 1.82-m Copernico telescope of Mt. Ekar, Asiago (Italy)]. North is up, east is to the left.

velocitys in the classification spectrum was found to be extremely low, roughly 500 km s^{-1} (Filippenko et al. 2004), as measured from the position of the absorption minima of the P Cygni profiles.

The adopted explosion epoch is JD = 245 3170 ± 30 inferred from the colour evolution (see Section 4.2). Main data of SN 2004eg and its host galaxy UGC 3053 are in Table 1.

2.4 SN 1999gn and SN 2006ov in M61

M61 (NGC 4303) is one of the largest galaxies in the Virgo cluster; its 6 arcmin diameter correspond to about 100 000 light years, similar to the diameter of the Milky Way. To date, 6 SNe have been registered in this galaxy: SN 1926A (Type IIL, mag 12.8), SN 1961I (Type II, mag 13), SN 1964F (Type I, mag 12), SN 1999gn and SN 2006ov (Fig. 4, Type IIP, this paper) and, more recently, the Type IIP SN 2008in (see Section 7). A Tully–Fisher distance $d = 12.6 \pm 2.4$ Mpc ($\mu = 30.5 \pm 0.4$) is adopted for M61, in agreement with Li et al. (2007) and Smartt et al. (2009).

SN 1999gn was discovered with a 0.50-m telescope by Dimai on 1999 December 17.22 UT at $\alpha = 12^{\mathrm{h}}21^{\mathrm{m}}57^{\mathrm{s}}02$, $\delta = +04°27'45''6$ (31.7 arcsec east and 39.8 arcsec south of the nucleus of the galaxy), when the object had magnitude 16.0. The new object was confirmed on the subsequent day through a KAIT image at a magnitude of about 15.5. The SN was clearly discovered in the rising phase to the maximum light (Dimai & Li 1999). In a KAIT image taken on November 26.5 no source was detected at the position of the transient to a limiting mag of about 19.0. The spectroscopic classification of SN 1999gn as Type II was assigned by Ayani & Yamaoka (1999) from a wide-band spectrum (range 400–800 nm, resolution 0.6 nm) obtained with the Bisei Astronomical Observatory 1.01-m telescope. The spectrum exhibited a blue continuum with overimposed broad Hα and Hβ P Cygni profiles. The expansion velocity of the SN was 5300 km s^{-1}, as derived from the position of the Hα absorption minimum (Ayani & Yamaoka 1999).

SN 2006ov was discovered by Nakano & Itagaki (Nakano, Itagaki & Kadota 2006) on 2006 November 24.86 UT with a 0.60-m reflector. The magnitude at discovery was 14.9. This object was located at
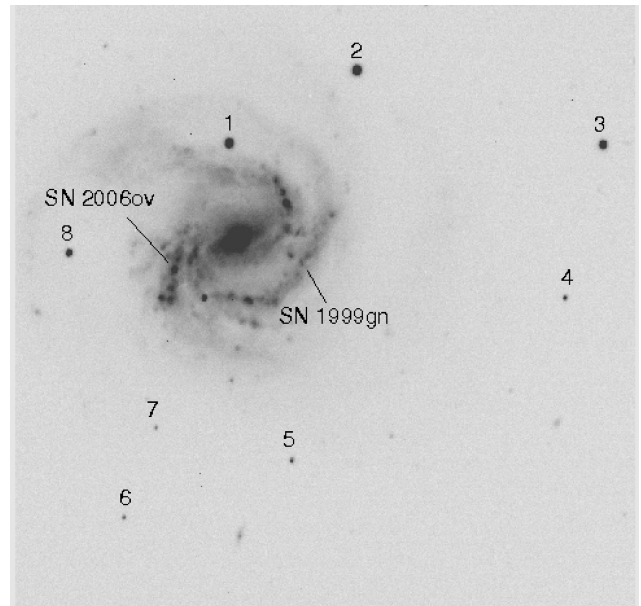

Figure 4. SN 2006ov and position of SN 1999gn in NGC 4303 [*V* band image obtained on 2006 December 20 with the Copernico 1.82-m telescope of Mt. Ekar, Asiago (Italy)]. The labels indicate the stars of the local sequence, as in Table 10. East is down, north is to the left.

$\alpha = 12^{\mathrm{h}}21^{\mathrm{m}}55^{\mathrm{s}}30$, $\delta = +04°29'16''7$ (equinox 2000.0), which is 5''5 east and 51'' north of the centre of the galaxy. Nothing was visible at this location on an exposure obtained on 2006 May 4 (to a limiting magnitude 19.5). Blondin et al. (2006) reported that a spectrogram (range 350–740 nm) of 2006ov obtained by Berlind on November 25.56 UT with the Whipple Observatory 1.5-m telescope (+ FAST), showed that SN 2006ov was a Type II SN roughly one month past explosion. Indeed the spectrum was similar to that of the Type IIP SN 2005cs at 36 d past explosion. Adopting a recessional velocity of 1570 km s^{-1} for the host galaxy (from 'The Updated Zwicky Catalog'), the absorption minimum of the Hα line (rest 656.3 nm) indicates an expansion velocity of 4000 km s^{-1} (Blondin et al. 2006).

The adopted explosion epochs are JD = 245 1520 ± 10 and JD = 245 3974 ± 6 for SN 1999gn and SN 2006ov, respectively, as inferred from spectroscopic and photometric information (see Section 4.2 and 5.1). Main data of SN 1999gn and SN 2006ov and their host galaxy are reported in Table 1.

3 SUMMARY OF THE OBSERVATIONS

In this paper we present new data for five SNe IIP for the first time, along with other data available in the literature. Images and spectra of the 5 SNe were obtained using the following instruments:

– the 1.82-m Copernico Telescope with AFOSC (Asiago-Mt. Ekar, Italy);
– the 0.8-m Teramo-Normale Telescope (TNT) with TK512CB1-1 CCD (Teramo, Italy);
– the ESO 3.6m with EFOSC2 (La Silla, Chile);
– the ESO 3.58-m New Technology Telescope (NTT) with EMMI (La Silla, Chile);
– the 2.3-m telescope at the Siding Spring Observatory (SSO) with DBS (Australia);
– the 74-inch telescope of the Mount Stromlo Observatory (MSO) plus B&C (Australia);

– the Calar Alto (CAHA) 2.2-m telescope with CAFOS (Calar Alto Observatory, Spain);

– the 2.5-m Irénée du Pont telescope plus WFCCD (Las Campanas Observatory, Chile);

– the 1.0-m Swope telescope (Las Campanas Observatory, Chile);

– the 2.0-m Faulkes Telescope (FT) north with HawkCam (Haleakala, Hawaii, USA);

– the 2.0-m MAGNUM with MIP (Haleakala, Hawaii, USA);[2]

– the 2.0-m Liverpool Telescope (LT) plus RATCam (La Palma, Spain);

– the 2.56-m Nordic Optical Telescope (NOT) plus ALFOSC (La Palma, Spain);

– the 4.2-m William Herschel Telescope (WHT) equipped with ISIS (La Palma, Spain);

– the 1.0m Jacobus Kapteyn Telescope (JKT) with JAG (La Palma, Spain);

– the 3.58-m Telescopio Nazionale Galileo (TNG) with Dolores (La Palma, Spain);

– the 0.41-m Newton Telescope (Nw 0.4m) of the Gruppo Astrofili di Padova (GAP) equipped with an Apogee AP47p CCD Camera (Padova, Italy).

After the usual initial (bias, overscan, normalized flat-fields) corrections, photometric data were reduced following standard prescriptions (see e.g. Pastorello et al. 2007) using tasks developed by the Asiago-Padova SN Group in the IRAF environment, while the spectroscopic data were reduced using traditional IRAF tasks. Two different methods were used to obtain the SN magnitudes: template subtraction and point spread function (PSF) – fitting technique, depending on the characteristics of the background where the SN exploded and/or the availability of pre-explosion images of the SN site in the given bands. The explosion epochs of all SNe of our sample were estimated through spectroscopic and photometric comparisons with the well-studied SN 2005cs for which the explosion date was well constrained (about 0.5 d; Pastorello et al. 2009). The underlying assumption is that LL SNe IIP have intrinsically similar properties (see Section 4.2).

4 LIGHT CURVES

Photometric data for SN 2002gd, SN 2003Z, SN 2004eg and SN 2006ov are presented here but we regret that no photometric follow up was performed for SN 1999gn.

4.1 Individual objects

4.1.1 SN 2002gd

The contribution of a large number of facilities allowed an extensive observational campaign for this SN during the photospheric phase in the optical bands. These are complemented by few near-infrared (NIR) data in the late plateau phase calibrated using the 2MASS catalogue (Skrutskie et al. 2006). Optical and NIR magnitudes of SN 2002gd are reported in Table 2 while the magnitudes of the local sequence stars (with associated errors) are in Table 3.

After the steep rise observed during the first few days after discovery, the SN reached the maximum in the optical bands around 2002 October 13. After the maximum the luminosity declined slightly in all bands (especially in *B*) for about 20 d. Then the SN entered the

plateau phase with a constant luminosity. The plateau of SN 2002gd lasted about three months, although a further minor rebrightening was observed at ∼70 d. The *U* band light curve had a different behaviour, showing a monotonic decline (see Fig. 5).

At about 110 d after the explosion, the SN luminosity dropped steeply, that usually takes the light curve to the radioactive tail. Unfortunately this transition was observed only in the initial phase because SN 2002gd was lost behind the Sun. We tried to recover the SN during the nebular phase but the SN was not visible and only upper limits in the SN luminosity were obtained.

These limits allow us to estimate an upper limit for the ^{56}Ni mass ejected in the explosion of SN 2002gd, that turned out to be very small, ≤ 0.003 M$_\odot$. Missing a real detection and, therefore, an estimate of the late-time magnitude decline rate, we cannot exclude a dimming of the luminosity due to dust formation into the ejecta that could lead us to underestimate the upper limit of the mass of ^{56}Ni.

4.1.2 SN 2003Z

Our photometric follow-up observations started about 1 month after the adopted explosion epoch and lasted until day 210, in the nebular phase. PSF-fitting photometric measurements of SN 2003Z are reported in Table 4, while the magnitudes of the sequence stars (Fig. 2) are listed in Table 5. Early-time photometry (both filtered and unfiltered) is adopted from the Bright Supernova website.[3] These data give useful constraints on the photometric evolution of the SN during the first month after the explosion and show that SN 2003Z was discovered when it was very young, likely a few days after the shock breakout. Merging these unfiltered measurements with those presented in this paper, allows us to infer a plateau duration of about 100 d (see Fig. 6). The end of the plateau is well determined, after which we observe a large luminosity drop lasting a few weeks, until the SN light curve reaches the exponential tail. Despite the relatively large uncertainty in the late-time photometry, the average luminosity decline is rather close to that expected for the luminosity decline of ^{56}Co into ^{56}Fe (0.98 mag/100 days, see Table 6).

4.1.3 SN 2004eg

Our optical photometry in the *g′BVRI* bands, collected in Table 7, span about 4 months. The sloan *r′* and *i′* magnitudes collected with the Swope telescope were converted into Johnson–Bessel *R* and *I* magnitudes making use of the relation presented in Smith et al. (2002):

$$V - R = 0.59(g' - r') + 0.11 \tag{1}$$

and

$$R - I = 1.00(r' - i') + 0.21 \text{(for } (r' - i') < 0.95). \tag{2}$$

Photometric measurements of SN 2004eg were performed using a PSF-fitting method. Photometric errors were estimated with artificial star experiments: the large errors are consistent with the faint SN magnitudes. For calibration we used the local stellar sequence shown in Fig. 3. Their magnitudes are reported in Table 8. The poorly sampled light curve of SN 2004eg is shown in Fig. 7. A few photometric points were collected in the plateau phase, and these allow us to estimate the SN luminosity in the recombination phase.

---

[2] Yoshii (2002) and Yoshii, Kobayashi & Minezaki (2003).

[3] http://www.rochesterastronomy.org

Table 2. Photometry of SN 2002gd.

Date	JD (240 0000+)	U	B	V	R	I	J	H	K	Instr.
					SN 2002gd					
08/10/02	525 55.52	–	–	–	17.40 (0.01)	–	–	–	–	1
08/10/02	525 55.55	16.25 (0.01)	17.51 (0.01)	17.33 (0.01)	17.38 (0.01)	17.33 (0.02)	–	–	–	1
10/10/02	525 57.66	–	17.43 (0.01)	17.21 (0.01)	17.14 (0.01)	17.08 (0.01)	–	–	–	2
10/10/02	525 57.67	–	–	–	17.14 (0.01)	–	–	–	–	2
10/10/02	525 58.04	16.36 (0.03)	17.43 (0.01)	17.19 (0.02)	17.07 (0.02)	17.01 (0.03)	–	–	–	3
10/10/02	525 58.04	–	17.46 (0.01)	–	–	–	–	–	–	3
12/10/02	525 60.04	–	–	17.10 (0.02)	16.95 (0.01)	16.90 (0.01)	–	–	–	3
13/10/02	525 61.02	–	–	17.08 (0.07)	16.90 (0.13)	16.82 (0.09)	–	–	–	3
14/10/02	525 61.93	–	–	17.14 (0.01)	–	–	–	–	–	3
14/10/02	525 61.95	16.77 (0.02)	17.54 (0.02)	17.13 (0.01)	16.96 (0.01)	16.91 (0.01)	–	–	–	3
18/10/02	525 66.41	–	–	17.13 (0.11)	–	–	–	–	–	4
24/10/02	525 72.34	–	–	17.34 (0.06)	17.03 (.06)	–	–	–	–	5
28/10/02	525 76.38	–	–	–	17.05 (0.12)	–	–	–	–	4
28/10/02	525 76.44	18.23 (0.05)	18.42 (0.02)	17.45 (0.02)	17.08 (0.02)	17.02 (0.02)	–	–	–	6
30/10/02	525 78.30	–	18.48 (0.12)	17.48 (0.08)	17.08 (0.09)	–	–	–	–	5
01/11/02	525 79.92	–	18.54 (0.03)	17.51 (0.02)	17.14 (0.02)	17.02 (0.02)	–	–	–	7
03/11/02	525 81.93	–	18.55 (0.11)	17.54 (0.03)	17.14 (0.02)	17.00 (0.02)	–	–	–	7
04/11/02	525 83.31	–	18.56 (0.15)	17.53 (0.03)	17.08 (0.05)	–	–	–	–	5
05/11/02	525 84.23	–	18.60 (0.04)	17.53 (0.02)	17.14 (0.02)	16.97 (0.04)	–	–	–	6
06/11/02	525 85.01	18.81 (0.17)	18.65 (0.04)	17.57 (0.04)	–	–	–	–	–	3
09/11/02	525 88.23	–	–	–	17.09 (0.20)	–	–	–	–	5
09/11/02	525 88.26	–	–	–	17.09 (0.10)	16.92 (0.08)	–	–	–	5
10/11/02	525 89.26	–	18.75 (0.20)	17.54 (0.11)	17.11 (0.04)	–	–	–	–	4
11/11/02	525 89.94	18.87 (0.33)	18.78 (0.04)	17.61 (0.03)	17.11 (0.02)	16.91 (0.02)	–	–	–	3
20/11/02	525 99.45	–	–	17.60 (0.04)	17.10 (0.04)	16.93 (0.10)	–	–	–	5
22/11/02	526 01.44	–	18.71 (0.08)	–	–	–	–	–	–	8
22/11/02	526 01.45	–	18.74 (0.08)	–	–	–	–	–	–	8
23/11/02	526 02.34	–	18.72 (0.10)	–	–	–	–	–	–	8
23/11/02	526 02.35	–	18.74 (0.13)	–	–	–	–	–	–	8
23/11/02	526 02.44	–	18.72 (0.28)	–	–	–	–	–	–	8
10/12/02	526 19.25	–	–	17.55 (0.12)	17.09 (0.04)	16.81 (0.02)	–	–	–	4
17/12/02	526 26.20	–	–	17.60 (0.05)	–	–	–	–	–	5
18/12/02	526 27.25	–	–	17.63 (0.09)	17.12 (0.03)	–	–	–	–	4
19/12/02	526 28.23	–	19.06 (0.10)	17.65 (0.05)	17.12 (0.05)	16.83 (0.17)	–	–	–	5
26/12/02	526 34.77	–	19.55 (0.03)	17.84 (0.02)	17.28 (0.02)	17.01 (0.02)	16.60 (0.04)	16.07 (0.05)	16.09 (0.04)	9
28/12/02	526 37.35	20.85 (0.30)	19.57 (0.04)	17.86 (0.02)	17.29 (0.02)	17.04 (0.04)	–	–	–	10
01/01/03	526 40.74	–	19.64 (0.03)	17.92 (0.02)	17.35 (0.02)	17.11 (0.02)	16.70 (0.06)	16.28 (0.04)	16.03 (0.08)	9
03/01/03	526 43.28	–	–	17.95 (0.05)	17.39 (0.05)	17.13 (0.05)	–	–	–	6
07/01/03	526 46.74	–	19.70 (0.03)	18.03 (0.03)	17.48 (0.02)	17.18 (0.02)	16.71 (0.04)	16.27 (0.06)	16.07 (0.07)	9
13/01/03	526 53.24	–	–	18.04 (0.14)	17.41 (0.12)	17.24 (0.30)	–	–	–	5
14/01/03	526 54.21	–	–	18.06 (0.03)	17.44 (0.03)	17.24 (0.03)	–	–	–	6
14/01/03	526 54.27	–	–	17.99 (0.08)	17.42 (0.08)	17.26 (0.13)	–	–	–	5
14/01/03	526 54.28	–	–	18.03 (0.11)	17.42 (0.15)	–	–	–	–	6
19/01/03	526 59.23	–	–	–	17.50 (0.05)	17.28 (0.03)	–	–	–	4
22/01/03	526 62.25	–	–	18.54 (0.11)	17.72 (0.20)	17.55 (0.07)	–	–	–	5
23/01/03	526 63.24	–	19.79 (0.09)	18.66 (0.06)	18.04 (0.03)	17.75 (0.02)	–	–	–	6
27/01/03	526 67.25	–	–	19.12 (0.30)	–	–	–	–	–	5
03/06/03	527 94.09	–	–	–	–	–	≥ 19.8	≥ 19.2	≥ 18.1	9
04/06/03	527 95.07	–	≥ 22.7	≥ 22.6	≥ 22.8	≥ 22.0	–	–	–	9
08/06/03	527 99.09	–	–	–	–	–	≥ 19.8	–	–	9
23/08/03	528 74.54	–	–	–	≥ 22.90	≥ 22.67	–	–	–	6

1 = ESO3.6m + EFOSC2; 2 = NTT + EMMI; 3 = SSO2.3m; 4 = Padova-Nw0.4m + CCD; 5 = TNT + CCD; 6 = Asiago1.82m + AFOSC; 7 = SSO-40inch + WFI; 8 = JKT + JAG; 9 = MAGNUM 2m + MIP; 10 = CAHA2.2m + CAFOS.

Additionally, a few photometric observations of the radioactive tail allow us to estimate the ^{56}Ni mass (see Section 4.3).
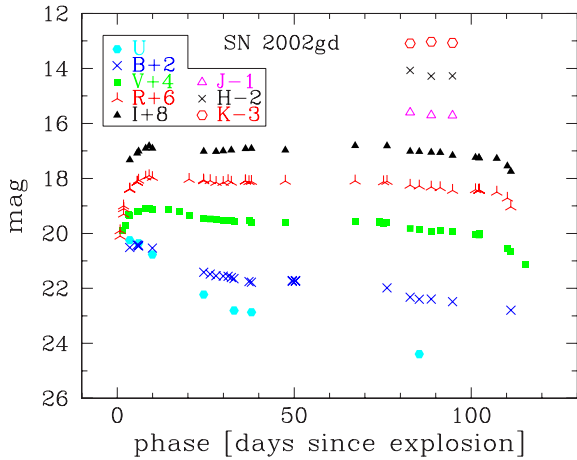
4.1.4 SN 2006ov

Photometric data were collected at 24 different epochs over a period of 150 d, starting from the end of the photospheric phase. SN magnitudes are reported in Table 9, while those of the local sequence stars used for the calibration are collected in Table 10. The light curve of SN 2006ov is shown in Fig. 8.

SN 2006ov exploded in a crowded background region of the host galaxy. As long as the source was bright, the SN data were obtained with the PSF-fitting technique. When the SN luminosity faded, the photometric measurements were performed using the template subtraction technique. The errors were estimated by putting artificial stars with the same magnitude as the SN, in a number of locations close to the SN position, and were estimated as the rms of the recovered magnitudes.

Unfortunately, this SN was discovered near the end of the plateau phase. A few points showed that in this phase the SN had a roughly

Table 3. Magnitudes of the local sequence stars in the fields of SN 2002gd.

Star	U	B	V	R	I
			SN 2002gd		
1	17.39 (0.05)	17.07 (0.02)	16.00 (0.02)	15.54 (0.02)	15.09 (0.01)
2	–	20.67 (0.05)	19.15 (0.03)	18.24 (0.02)	17.29 (0.02)
3	–	21.40 (0.09)	19.80 (0.05)	18.65 (0.03)	17.55 (0.03)
4	–	19.26 (0.04)	17.67 (0.02)	16.80 (0.02)	15.98 (0.01)
5	18.35 (0.10)	17.43 (0.02)	16.05 (0.01)	15.35 (0.01)	14.71 (0.02)
6	–	21.63 (0.07)	19.83 (0.04)	18.72 (0.03)	17.48 (0.02)
7	–	20.39 (0.05)	19.66 (0.05)	19.36 (0.05)	18.86 (0.04)
8	17.54 (0.05)	17.67 (0.02)	16.85 (0.02)	16.52 (0.01)	16.18 (0.01)
9	19.03 (0.20)	19.73 (0.04)	19.26 (0.03)	19.18 (0.04)	18.94 (0.03)

Figure 5. Early-time *UBVRIJHK* light curves of SN 2002gd.

constant magnitude, about $m_V \simeq 15.7$ mag. Between day ∼110 and day ∼140, after the end of the recombination phase, a steep decline of more than 4 mag was observed in all bands. A slower decline is then observable beyond 150 d. In this phase, the SN becomes too faint to be observed in the *B* band and only upper limits were measured. Nevertheless, the luminosity decline at late epochs is still consistent with the radioactive decay of ^{56}Co into ^{56}Fe (Section 4.3).

4.2 Colour curves

In this section we compare the colour curves of an extensive sample of underluminous SNe IIP, including the objects discussed in the previous sections (SN 2002gd, SN 2003Z, SN 2004eg and SN 2006ov) together with SN 1994N, SN 1999br, SN 1999eu, SN 2001dc (Pastorello et al. 2004), SN 1997D (Turatto et al. 1998; Benetti et al. 2001), SN 2005cs (Pastorello et al. 2006, 2009; Tsvetkov et al. 2006; Brown et al. 2007), SN 2008bk (Van Dyk et al. 2012), SN 2008in (Roy et al. 2011), SN 2009N (Takáts et al. 2014), SN 2009md (Fraser et al. 2011) and SN 2010id (Gal-Yam et al. 2011).

The explosion epochs for the whole SN sample were computed mainly using the available photometric information, and dating the available SN spectra. In the case of SN 2003Z and SN 2002gd, both well sampled during early stages, the explosion epochs have been calculated by comparing the evolution of the light curves with those of SN 2005cs. Additional information is provided from the early rising branch and pre-SN detection limits. In the case of SN 2004eg and SN 2006ov, for which we have a less complete photometric coverage, we dated the explosions making use of the homogeneity

of the $(B - V)$ and $(V - R)$ colour curves (Pastorello et al. 2004) and of the spectroscopic evolution (Section 5).

The $(B - V)$ and $(V - R)$ colour curves during the first 120 d are shown in Fig. 9. Only corrections for Galactic extinctions have been applied to the whole sample except for the cases of SN 2005cs in which the (small) host galaxy extinction is well constrained ($A_{B,\text{tot}} = 0.205$ mag; see Pastorello et al. 2009) and SN 2001dc whose colours indicate significant interstellar reddening. This feature, together with the fact that SN 2001dc exploded in a dusty region of the host galaxy, lead us to correct its colour for internal extinction as in Pastorello et al. (2004) ($A_{B,i} = 1.654$ mag, $A_{B,\text{tot}} = 1.693$ mag).

During the photospheric phase, following the envelope expansion and cooling, the $(B - V)$ colour reddens during the first 60 d reaching $(B - V) \simeq 1.4$ mag, then it remains around this value for the subsequent 60 d (when the H envelope recombines). The $(V - R)$ colour, reaches $\simeq 0.6$ mag at about 70 d, followed by a flattening in the subsequent period. A red spike is visible at ∼120 d.

The high degree of homogeneity in the colours of these objects during the first 100 d might suggest some homogeneity in the properties of the progenitor stars.

At about 4 months past CC a larger dispersion in the $(B - V)$ colour is visible among faint SNe IIP. A similar behaviour is observed for the $(V - R)$ colour, ranging from $(V - R) \simeq 0.4$ mag in the case of SN 2004eg to $(V - R) \simeq 0.8$ mag in the case of SN 2006ov. This is mostly due to the intrinsic faintness of the SNe in this phase, that increases significantly the photometric errors.

4.3 Bolometric light curves

Pseudo-bolometric light curves for our SN sample were obtained by integrating the fluxes in the *B, V, R, I* bands (Fig. 10). As a reference object, we also consider the *BVRI* pseudo-bolometric light curve of the normal Type IIP SN 2004et. It is evident that the bolometric luminosities of all objects in our sample are systematically fainter than that of SN 2004et, and – in particular – their plateau luminosities are at least a factor of ×10 fainter. As mentioned in previous sections, the plateau phase in subluminous SNe IIP lasts about 100–110 d, followed by an abrupt drop by about 3–5 mag, when the SN light curves settle on to the much slower radioactive tail powered primarily by the radioactive decay of Co to Fe.

Despite the general homogeneity in the photometric properties, some interesting and significant differences are visible among the objects.

The luminosity of the plateau in our sample range between the upper value of SN 2009N ($L_{BVRI} \approx 2.8 \times 10^{41}$ erg s^{-1}), and the lower extreme marked by SN 1999br, $L_{BVRI} \approx 3.5 \times 10^{40}$ erg s^{-1}.

Table 4. Photometry in the optical bands of SN 2003Z. The data have been obtained using several telescopes in Italy and Canary Islands (Spain).

Date	JD (240 0000+)	U	B	V	R	I	Ins.
			SN 2003Z				
21/02/03	526 92.40	–	–	–	17.03 (0.05)	–	1
21/02/03	526 92.44	–	18.12 (0.02)	17.33 (0.03)	–	16.81 (0.02)	1
23/02/03	526 94.41	18.84 (0.06)	18.16 (0.05)	17.31 (0.04)	16.98 (0.02)	16.74 (0.02)	2
05/03/03	527 04.40	–	18.43 (0.06)	–	–	–	2
05/03/03	527 04.41	–	18.43 (0.12)	–	–	–	2
05/03/03	527 04.42	–	18.42 (0.10)	–	–	–	2
05/03/03	527 04.43	–	18.43 (0.07)	17.44 (0.04)	16.96 (0.04)	16.65 (0.02)	2
27/03/03	527 26.32	–	18.86 (0.07)	17.48 (0.02)	16.97 (0.03)	16.57 (0.02)	2
08/04/03	527 38.41	–	18.92 (0.15)	17.52 (0.05)	16.98 (0.03)	16.56 (0.03)	2
10/04/03	527 39.50	–	19.04 (0.05)	17.52 (0.01)	17.04 (0.01)	16.67 (0.01)	1
13/04/03	527 43.40	–	–	17.52 (0.11)	17.03 (0.07)	–	3
16/04/03	527 46.36	–	–	17.53 (0.16)	17.03 (0.07)	–	3
29/04/03	527 59.36	–	–	17.61 (0.07)	17.15 (0.08)	–	3
01/05/03	527 61.46	–	19.33 (0.08)	17.67 (0.03)	17.19 (0.02)	16.83 (0.02)	1
07/05/03	527 67.43	–	19.40 (0.26)	17.86 (0.10)	17.23 (0.09)	16.83 (0.14)	2
07/05/03	527 67.45	–	–	–	–	16.85 (0.09)	2
08/05/03	527 68.42	–	19.43 (0.06)	17.87 (0.04)	17.29 (0.03)	16.89 (0.02)	2
11/05/03	527 71.38	–	–	17.86 (0.08)	17.30 (0.14)	17.03 (0.06)	3
21/05/03	527 81.46	–	–	17.94 (0.07)	17.43 (0.07)	–	3
23/05/03	527 83.38	–	19.75 (0.23)	18.24 (0.07)	–	–	2
23/05/03	527 83.40	–	19.76 (0.25)	–	17.65 (0.13)	17.29 (0.09)	2
26/06/03	528 17.41	–	22.13 (0.28)	20.31 (0.11)	19.41 (0.05)	18.90 (0.04)	1
21/07/03	528 41.36	–	–	20.47 (0.32)	19.66 (0.23)	19.04 (0.15)	2
23/08/03	528 74.63	–	–	–	20.07 (0.15)	19.15 (0.21)	2

1 = TNG + Dolores; 2 = Asiago 1.82m + AFOSC; 3 = Nw 0.4m + CCD.

Table 5. Magnitudes of the stars of the local sequences of SN 2003Z. The numbers in brackets are the rms of the available measurements. If no error is reported, only a single estimate is available.

Star	U	B	V	R	I
			SN 2003Z		
1	–	18.87 (0.03)	17.65 (0.01)	16.89 (0.02)	16.26 (0.01)
2	18.08 (–)	17.35 (0.01)	16.43 (0.01)	16.00 (0.01)	15.54 (0.01)
3	–	19.03 (0.01)	17.53 (0.01)	16.59 (0.01)	15.62 (0.01)
4	14.13 (–)	13.88 (–)	13.29 (0.03)	12.93 (0.02)	–
5	14.32 (–)	14.04 (–)	13.41 (0.03)	13.05 (0.02)	–
6	–	17.44 (0.02)	16.79 (0.01)	16.41 (0.01)	16.06 (0.01)
7	–	18.19 (0.02)	16.98 (0.01)	16.13 (0.01)	15.37 (0.01)
8	–	–	16.84 (0.12)	16.14 (0.01)	–
9	–	17.76 (–)	16.63 (0.05)	15.89 (0.02)	15.06 (–)
10	19.75 (–)	18.40 (0.02)	17.28 (0.02)	16.52 (0.01)	15.73 (0.02)
11	–	–	13.41 (–)	13.07 (0.02)	–
12	–	15.71 (–)	14.99 (–)	14.69 (0.03)	14.20 (–)
13	–	–	16.85 (–)	16.14 (0.05)	–
14	15.95 (–)	–	14.68 (–)	14.22 (0.02)	13.69 (0.01)
15	–	–	15.62 (–)	15.25 (0.04)	–
16	–	18.72 (0.09)	18.14 (0.01)	17.82 (0.01)	17.39 (0.01)
17	–	18.82 (0.02)	18.18 (0.01)	17.80 (0.01)	17.41 (0.01)
18	–	19.67 (0.02)	18.29 (0.01)	17.37 (0.01)	16.60 (0.01)

This wide range in the plateau luminosity suggests some differences in the kinematics of the expanding gas, in the initial radius or in the masses of the hydrogen envelope, where the recombination takes place (or a combination of them).

Between days 150 and 500 all light curves show a similar behaviour, with nearly linear luminosity declines, consistent with that expected from the radioactive decay of ^{56}Co into ^{56}Fe (0.98 mag/100 days). During this phase, at around 400 d, we ob-

serve a spread in the luminosity of the sample between the lower value of SN 1999br and SN 1999eu ($L_{BVRI} \approx 4 \times 10^{38}$ erg s^{-1}) and the higher value of SN 2009N ($L_{BVRI} \approx 4 \times 10^{39}$ erg s^{-1}). This is an indication of a significant spread in the ^{56}Ni masses ejected by LL SNe IIP.

Through a comparison with the late-time luminosity of SN 1987A we could estimate the ^{56}Ni masses for all objects of our SN sample. We found values spanning from 1×10^{-3} up to 2×10^{-2} M$_{\odot}$(Ni),
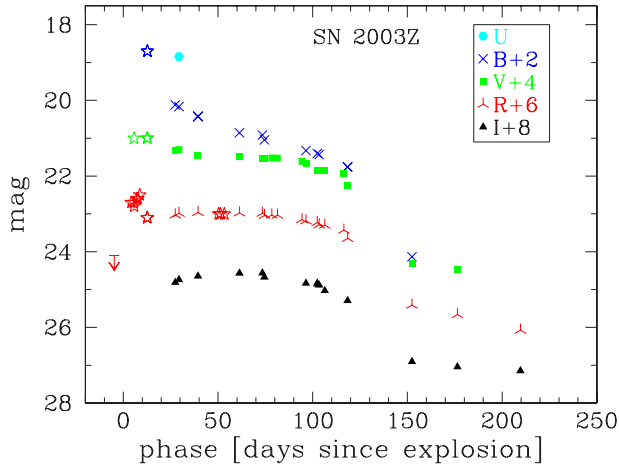
Figure 6. *UBVRI* light curves of SN 2003Z. The unfiltered pre-discovery limit is shown with respect to the *R* magnitude scale. Open star symbols are filtered magnitudes from http://www.rochesterastronomy.org (measured by Gary), all other symbols represent magnitudes published in this paper.

Table 6. Slopes of the light curves of SN 2003Z in the *B, V, R, I* bands (in mag/100^d). The phase is relative to the explosion date (JD = 245 2665).

Band	10–40^d	35–100^d	90–110^d	115–155^d	$\geq 150^d$
γ_B	6.32^a	1.60	1.44	6.99	–
γ_V	1.73	0.36	2.32	6.37	0.67
γ_R	-0.54	0.32	1.21	5.37	1.05
γ_I	-1.20	0.31	1.68	4.73	0.58

^{a}The measured slope of the *B* band light curve changes from $\gamma_B = 9.65$ (10–30 d) to $\gamma_B = 2.58$ (25–40 d).

1–2 orders of magnitude less than in normal SNe IIP (for more details, see Section 6).

5 SPECTROSCOPY

In this section we present the spectroscopic evolution of the five underluminous SNe IIP introduced in the previous sections. SN 2002gd, SN 2003Z and SN 2006ov have been well monitored, whilst for SN 1999gn and SN 2004eg only one and two spectra are available, respectively. The journal of spectroscopic observation is presented in Table 11.

Table 7. Photometry in the optical bands of SN 2004eg. The data of this SN have been obtained using TNG, Swope and Asiago 1.82-m telescopes.

Date	JD (2400000+)	g'	B	V	R	I	Ins.
				SN 2004eg			
08/09/04	53256.91	–	21.02 (0.09)	–	–	–	1
09/09/04	53257.89	19.89 (0.03)	–	–	18.13 (0.03)	17.47 (0.03)	1
11/09/04	53259.89	19.68 (0.04)	–	19.06 (0.04)	18.13 (0.03)	17.50 (0.03)	1
12/09/04	53260.89	–	20.76 (0.07)	–	–	–	1
13/09/04	53261.89	19.97 (0.04)	–	19.22 (0.04)	18.26 (0.04)	17.57 (0.04)	1
14/09/04	53262.85	19.95 (0.04)	–	19.19 (0.04)	18.22 (0.04)	17.55 (0.04)	1
11/11/04	53321.69	–	–	22.35 (0.33)	20.91 (0.09)	20.05 (0.10)	2
16/11/04	53327.48	–	–	22.42 (0.25)	20.94 (0.20)	20.16 (0.32)	3
15/12/04	53355.43	–	–	22.52 (0.36)	21.20 (0.13)	20.41 (0.11)	3
03/01/05	53375.42	–	–	22.53 (0.36)	21.35 (0.22)	20.57 (0.19)	3

1 = Swope; 2 = TNG + Dolores; 3 = Asiago 1.82m + AFOSC.

Table 8. Magnitudes of the stars of the local sequence. The numbers in brackets are the rms of the available measurements. If no error is reported, only a single estimate is available.

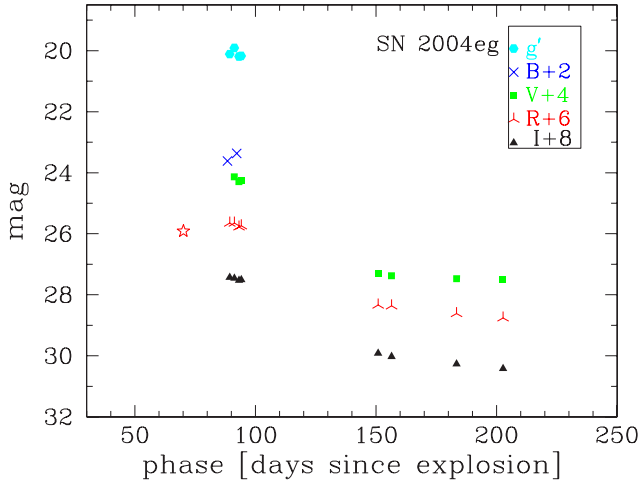| Star	g'	B	V	R	I
			SN 2004eg		
1	18.00 (0.01)	18.40 (0.03)	17.69 (0.02)	17.14 (0.02)	16.62 (0.02)
2	18.35 (0.01)	18.92 (0.01)	17.88 (0.02)	17.23 (0.03)	16.58 (0.01)
3	–	–	18.42 (0.02)	17.79 (0.03)	17.27 (0.01)
4	18.59 (0.01)	19.02 (0.05)	18.27 (0.01)	17.72 (0.02)	17.20 (0.01)
5	18.13 (0.01)	18.50 (0.04)	17.85 (0.02)	17.34 (0.02)	16.82 (0.01)
6	–	–	16.49 (0.02)	15.90 (0.01)	15.31 (0.06)
7	–	–	15.72 (0.02)	15.21 (0.03)	14.70 (–)
8	–	–	18.22 (0.01)	17.62 (0.03)	17.04 (0.01)
9	–	–	17.48 (0.01)	16.98 (0.04)	16.45 (0.01)
10	–	–	15.82 (0.02)	15.05 (0.03)	–
11	–	–	18.15 (0.01)	17.29 (0.01)	16.66 (–)
12	–	–	18.34 (0.05)	17.44 (0.06)	16.65 (–)
13	–	–	17.29 (0.05)	16.51 (0.06)	15.88 (–)
14	–	–	16.75 (0.04)	16.21 (0.07)	15.73 (–)

Figure 7. *g'BVRI* light curves of SN 2004eg. The open symbol is from Young et al. (2004), filled ones are magnitudes published in this paper.

5.1 Individual properties

(i) *SN 1999gn*. Only one spectrum of SN 1999gn is available (Fig. 11, top) taken during the plateau phase. By comparing this spectra with a library of SN spectra via GELATO (Harutyunyan et al. 2008) we could estimate a phase of about 45 d past explosion. The continuum is red and is characterized by the presence of a number of P Cygni lines, including Hα, Sc II 5527 Å, Na I D 5890,

Table 10. Magnitudes of the stars of the local sequences. The numbers in brackets are the rms of the available measurements. If no error is reported, only a single estimate is available. Due to the large rms star n.3 was not used for the calibration.

Star	B	V	R	I
		SN 2006ov		
1	15.22 (0.01)	14.27 (0.01)	13.65 (0.01)	13.14 (0.02)
2	14.56 (0.02)	13.98 (0.01)	13.60 (0.01)	13.24 (0.04)
3	15.98 (0.58)	15.43 (0.70)	14.92 (0.58)	14.58 (0.56)
4	18.26 (–)	16.95 (–)	16.17 (–)	15.48 (–)
5	18.78 (0.03)	17.55 (0.01)	16.80 (0.02)	16.07 (0.03)
6	18.23 (0.04)	17.59 (0.02)	17.24 (0.04)	16.84 (0.02)
7	19.43 (0.03)	18.10 (0.04)	17.07 (0.01)	16.19 (0.01)
8	16.68 (0.02)	15.59 (0.01)	14.85 (0.01)	14.19 (0.01)

5896 Å, Ba II (multiplet 1 at 4554, 4934 Å and multiplet 2 at 5854, 6142, 6497 Å), Fe II, O I, Ca II, Ti II and Cr II (see Pastorello et al. 2004 for a detailed line identification). The velocity inferred from Sc II 6246 Å line is v (Sc II) = 1690 ± 100 km s^{-1}, significantly lower than that observed in normal Type II SNe, and close to the value inferred for SN 2005cs at a similar epoch (v = 1550 km s^{-1}; Pastorello et al. 2009).

(ii) *SN 2002gd*. We extensively monitored SN 2002gd, especially during the photospheric phase (Fig. 12). The two earliest spectra, obtained with the ESO 4-m class telescopes have the best signal-to-noise (S/N) ratio and are dominated by a blue continuum and only Balmer lines and He I λ5876 Å are detected. In addition, a

Table 9. New photometry in the optical bands for SN 2006ov.

Date	JD (2400000+)	B	V	R	I	Ins.
			SN 2006ov			
24/11/06	54064.34	–	–	14.90 (–)	–	6
28/11/06	54067.70	17.16 (0.08)	15.73 (0.03)	15.09 (0.02)	14.72 (0.02)	1
05/12/06	54074.73	17.16 (0.03)	15.74 (0.02)	15.13 (0.01)	14.80 (0.01)	2
15/12/06	54084.71	17.46 (0.05)	16.00 (0.02)	15.21 (0.01)	14.91 (0.01)	2
15/12/06	54085.11	17.50 (0.04)	15.99 (0.02)	15.28 (0.02)	–	4
20/12/06	54089.72	17.70 (0.14)	16.24 (0.04)	15.55 (0.03)	15.11 (0.03)	1
20/12/06	54090.04	17.69 (0.05)	16.29 (0.01)	15.49 (0.01)	–	4
21/12/06	54091.11	17.96 (0.02)	16.43 (0.01)	15.62 (0.01)	–	4
30/12/06	54099.62	≥21.23	19.55 (0.15)	17.56 (0.05)	17.47 (0.11)	2
20/01/07	54120.67	–	20.04 (0.06)	18.58 (0.02)	18.25 (0.07)	2
21/01/07	54121.67	–	20.04 (0.18)	18.82 (0.06)	18.24 (0.07)	2
22/01/07	54122.56	–	20.01 (0.10)	18.77 (0.07)	18.23 (0.07)	2
22/01/07	54122.67	–	19.93 (0.23)	18.87 (0.02)	18.27 (0.10)	2
25/01/07	54126.05	≥20.81	19.99 (0.21)	18.73 (0.04)	–	4
25/01/07	54126.11	≥20.89	19.89 (0.22)	18.88 (0.07)	–	4
10/02/07	54141.56	–	20.15 (0.26)	19.12 (0.02)	18.66 (0.07)	2
11/02/07	54142.76	–	20.02 (0.25)	19.16 (0.06)	18.72 (0.12)	3
12/02/07	54144.12	≥20.87	20.01 (0.13)	18.98 (0.17)	–	4
12/02/07	54144.59	–	20.15 (0.11)	19.18 (0.03)	18.72 (0.15)	2
13/02/07	54144.91	≥20.60	20.21 (0.21)	18.97 (0.05)	–	4
13/02/07	54145.03	≥21.61	20.19 (0.15)	19.09 (0.16)	–	4
16/02/07	54147.92	≥20.65	19.97 (0.18)	19.02 (0.16)	–	4
16/02/07	54148.05	≥20.09	20.11 (0.40)	19.11 (0.18)	–	4
22/02/07	54154.05	≥20.57	20.08 (0.22)	19.24 (0.13)	–	4
08/03/07	54168.07	–	≥19.83	19.45 (0.13)	–	4
11/03/07	54171.57	–	20.20 (0.26)	19.48 (0.20)	18.85 (0.02)	5
21/03/07	54181.04	≥20.16	≥19.99	19.53 (0.35)	–	4
24/03/07	54183.95	≥20.94	20.29 (0.63)	19.43 (0.03)	–	4
15/04/07	54206.45	≥21.10	20.23 (0.06)	19.74 (0.14)	19.26 (0.09)	1

1 = Asiago 1.82m + AFOSC; 2 = LT; 3 = NOT; 4 = FT north; 5 = WHT; 6 = Nakano et al. (2006).
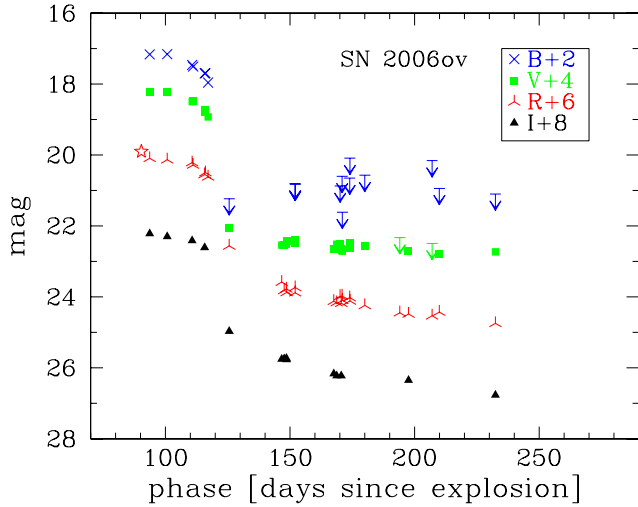
Figure 8. *BVRI* light curves of SN 2006ov. The open symbol is the unfiltered discovery magnitude (Nakano et al. 2006) showed with respect to the *R* band. Filled ones are magnitudes published in this paper.
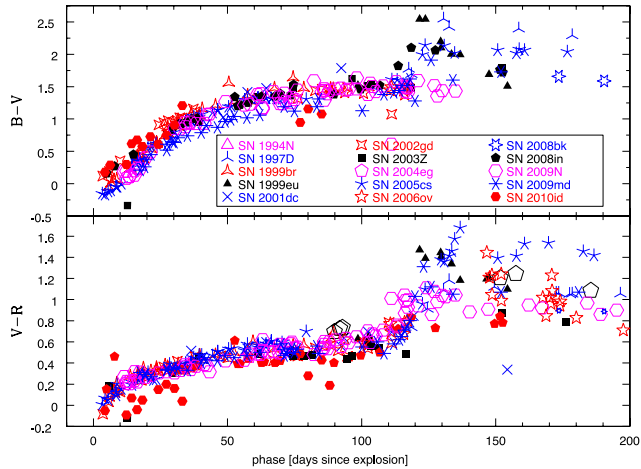

Figure 9. Evolution of $(B - V)$ and $(V - R)$ colours during the photospheric phase for the SNe of our sample.
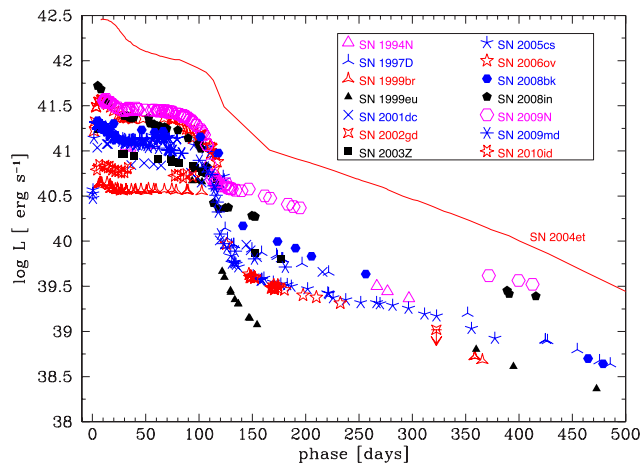

Figure 10. BVRI bolometric light curves for our LL SN IIP sample.

P Cygni profile is detected at about 6250 Å, possibly identified as Si II 6355 Å. When the temperature fades, Fe II and Ca II lines begin to appear and He I is replaced by the Na I doublet. Between days 30 and 40 after explosion, other metal lines with P Cygni profiles become prominent, including O I, Ti II, Sc II, Sr II, Ba II and Cr II. The line blanketing at the short wavelengths increases and the continuum becomes redder: this is consistent with the colour evolution discussed above. In late-photospheric spectra, Hα, Na I D and Ca II are the most prominent spectral features.

(iii) *SN 2003Z*. The first four spectra presented in Fig. 13 are from Knop et al. (2007) and display the early evolution of this SN. We started our monitoring about ~ 1 month after the discovery. The early spectra show relatively strong P Cygni lines of H, Ca II, Na I and Fe II, while other metal lines, such as Sc II, Ba II, Cr II and Ti II become prominent during the plateau phase. The sequence of spectra of this SN is one of the most comprehensive among LL events. It covers the transition from early spectra (similar to those of canonical Type II SNe) to the end of the plateau. At which point the spectra have red continua and prominent, very narrow P Cygni lines.

(iv) *SN 2004eg*. Two spectra are available for SN 2004eg (Fig. 11), one at the end of the plateau phase and one in the nebular phase. The first spectrum (+93 d) shows extremely narrow lines with P Cygni profiles: Sc II 5527 Å, Ba II 6142 Å, Na I 5890, 5896 Å and Ca II H&K and NIR triplet (8498, 8542, 8662 Å) are detected. In the nebular spectrum (+171 d) besides Hα and Na I D the most prominent lines are identified as [Ca II] 7291, 7324 Å, O I 7774 Å and Ca II NIR triplet. Hα and Ca II lines present asymmetric profiles with two components: one with a higher full width at half-maximum (FWHM), from which we inferred a velocity $v \sim 1400$–1500 km s^{-1}, and a narrow marginally resolved component of lower velocity, $v \sim 600$–850 km s^{-1}. We note that the [O I] lines (6300, 6364 Å) are very weak in the December 1 spectrum. Jerkstrand et al. (2012) and Maguire et al. (2012) suggest that high progenitor mass stars (~ 19 M$_\odot$) produce about a factor of 2 more oxygen during their nucelosynthesis than low-mass ones ($M \leq 15$ M$_\odot$), hence weakness (or total absence) of these lines supports the arguments for a lower mass progenitor for SN 2004eg (see Section 7).

(v) *SN 2006ov*. We collected five spectra of SN 2006ov (see Fig. 14): one at the end of the plateau phase (+93 d), two during the post plateau drop (+115 d and +121 d) and two in the nebular phase (+168 d and +197 d).

The continuum at 93 d is red and many narrow P Cygni lines are visible: H Balmer lines, O I 7774, Ca II, Ba II (multiplet 1 at 4554, 4934 Å and multiplet 2 at 5854, 6142, 6497 Å), Sc II, Ti II and Cr II (for details see Section 5.2), along with Na I D absorption features at 5890, 5896 Å. The velocities inferred from Hα and Sc II lines in this phase are $v(\mathrm{H}\alpha) \sim 3320$ km s^{-1} and $v(\mathrm{Sc\ II}) \sim 1310$ km s^{-1} (Fig. 15). The velocity $v(\mathrm{H}\alpha)$ is significantly lower than that measured in normal SNe IIP, but at the same time is relatively high when compared with that of other LL SNe IIP at a similar phase ($v(\mathrm{H}\alpha) = 1070, 1190, 1130$ km s^{-1} for SN 1999eu, SN 2001dc and SN 2003Z, respectively). This effect in SN2006ov is probably due to Hα being blended with other lines, including Ba II 6497 Å.

The spectra in the post-plateau phase show even redder continua, in agreement with the colour evolution discussed above. In this phase the gradual fading of permitted P Cygni metal lines is observed, with forbidden emission lines, such as [O I], [Fe I], [Fe II] and [Ca II], becoming more prominent with time.

Table 11. Journal of spectroscopic observations.

Date	JD (240 0000+)	Phase (d)	Instrument	Grism	Range (A)	Res. (A)
			SN 1999gn			
21/01/2000	515 64.77	45.7	NTT+EMMI	gm2+gm4	3900–10600	24 + 37
			SN 2002gd			
08/10/2002	525 55.53	3.5	ESO 3.6M+EFOSC2	gm11+gm12	3330–9990	12 + 11
10/10/2002	525 57.69	5.7	ESO NTT+EMMI	gm3	3720–9060	8
10/10/2002	525 58.08	6.1	SSO 2.3m+DBS	–	3300–4270, 5790–6750	1.1 + 1.1
13/10/2002	525 61.06	9.1	SSO 2.3m+DBS	–	3040–9140	5 + 8
14/10/2002	525 62.03	10.0	SSO 2.3m+DBS	–	3160–9140	5 + 8
23/10/2002	525 71.0	19.0	MSO 74in+B&C	300 l/mm grating	3870–7390	8
28/10/2002	525 76.37	24.4	Asiago 1.82m+AFOSC	gm4	3400–7760	24
05/11/2002	525 84.33	32.3	Asiago 1.82m+AFOSC	gm4	3390–7770	24
12/11/2002	525 90.76	38.8	SSO 2.3m+DBS	–	3450–9110	5
28/11/2002	526 07.46	55.5	CAHA 2.2m+CAFOS	B200	3200–8150	13
28/12/2002	526 37.31	85.3	CAHA 2.2m+CAFOS	B200	3240–8780	13
03/01/2003	526 43.26	91.3	Asiago 1.82m+AFOSC	gm4	3390–7760	24
14/01/2003	526 54.27	102.3	Asiago 1.82m+AFOSC	gm4	4310–7650	24
24/01/2003	526 64.27	112.3	Asiago 1.82m+AFOSC	gm4	3400–7760	24
			SN 2003Z			
21/02/2003	526 92.48	27.5	TNG+LRS	LR-B	3160–8050	16
24/02/2003	526 94.54	29.5	Asiago 1.82m+AFOSC	gm2+gm4	3400–9070	24 + 38
04/03/2003	527 02.57	37.6	Asiago 1.82m+AFOSC	gm4	3580–7820	24
06/03/2003	527 04.51	39.5	Asiago 1.82m+AFOSC	gm4	3590–7810	24
08/04/2003	527 38.36	73.4	Asiago 1.82m+AFOSC	gm4	3560–7760	24
10/04/2003	527 39.55	74.6	TNG+LRS	LR-B	3190–8030	16
01/05/2003	527 61.49	96.5	TNG+LRS	LR-B	3200–8030	16
08/05/2003	527 68.45	103.5	Asiago 1.82m+AFOSC	gr4	3410–7750	24
27/06/2003	528 18.41	153.4	TNG+LRS	LR-B	3200–8030	16
			SN 2004eg			
14/09/2004	532 63	93	DuPont+WFCCD	–	3800–9200	–
01/12/2004	533 41.56	171.6	TNG+Dolores	LR-R	4886–9016	12
			SN 2006ov			
28/11/2006	540 67.72	93.7	Asiago 1.82m+AFOSC	gm2+gm4	3400–9070	24 + 38
20/12/2006	540 89.71	115.7	Asiago 1.82m+AFOSC	gm2+gm4	3400–9070	24 + 38
26/12/2006	540 95.75	121.7	WHT+ISIS	R158R+R300B	3076–9597	6 + 9
11/02/2007	541 42.73	168.7	NOT+ALFOSC	gm5	4906–9759	16
12/03/2007	541 71.72	197.7	WHT+ISIS	R158R+R300B	3048–10458	6 + 9

As the SN ages, the main spectral features become [Ca II] doublet 7291, 7323 Å, Ca II IR triplet 8498, 8542, 8662 Å and [O I] 6300, 6364 Å. Noticeably, O I 7774 remains particularly prominent.

5.2 Common spectral properties in LL SNe IIP

On the basis of the data set presented here and in previous papers (Turatto et al. 1998; Benetti et al. 2001; Pastorello et al. 2004, 2006, 2009), we investigate the general spectral properties of an extensive sample of LL SNe IIP.

Phase $\lesssim 30$ d. The evolution of LL SNe IIP during the early photospheric phase is well illustrated by the spectral sequences of SN 2002gd and SN 2003Z. During the first 2–3 weeks, the spectra of LL SNe IIP are dominated by a blue continuum and only Balmer H lines and He I 5876 Å are detectable, showing relatively weak and shallow P Cygni profiles. Afterwards, Ca II H&K lines (3934, 3968 Å), Fe II (especially the lines of the multiplet 42 at 4924, 5018 and 5169 Å), O I 7774 Å and the Ca II infrared triplet (8498, 8542 and 8662 Å) become prominent, while He I 5876 Å disappears

being replaced by Na I D (5890, 5896 Å). The qualitative spectral evolution of these LL SNe during this period is similar to that of SNe IIP with higher luminosities and kinetic energies.

We measured the expansion velocities of the ejecta from the position of the absorption minima of both Hα and Sc II 6246 Å lines, and the temperatures via blackbody fits to the spectral continuum over regions not affected by line blanketing. The inferred values are reported in Table 12. During the first weeks after CC the photospheric velocity, inferred from the Sc II 6246 Å minimum (Fig. 15, bottom panel), rapidly decreases, reaching ∼4000 km s^{-1} at about two weeks and ∼2000 km s^{-1} at ∼30 d. Fig. 15 illustrates the expansion velocity of the normal SN IIP SN 2004et (Maguire et al. 2010) for comparison. It is evident that the expansion velocities of LL SNe are lower at any epoch by a factor of 2–3 than those of SN 2004et.

The temperature evolution is shown in Fig. 15 (top panel) for the whole sample of LL SNe IIP. As a reference we plot the temperature evolution of the normal Type IIP event SN 2004et (Maguire et al. 2010). With age, the continuum, which is initially
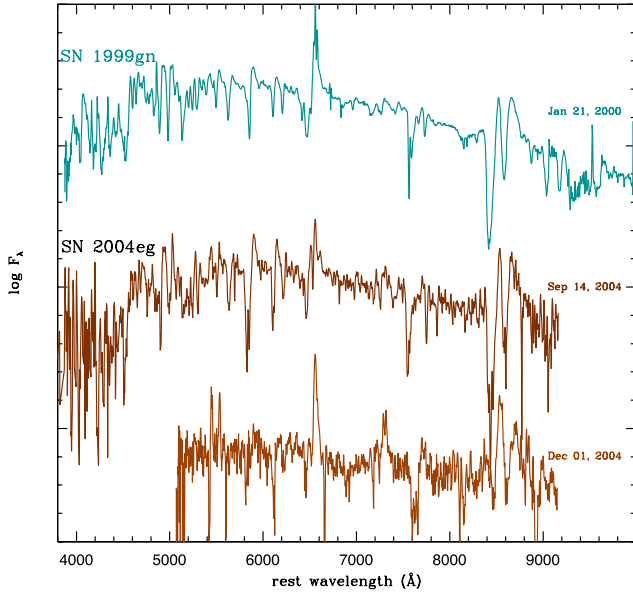
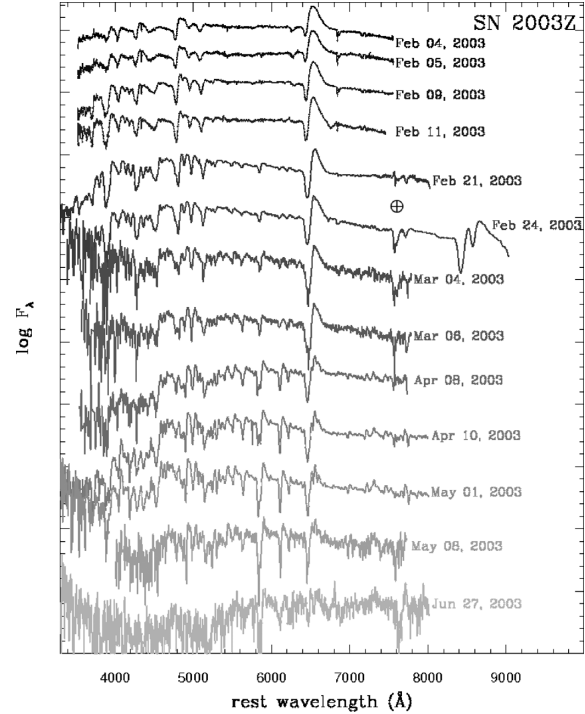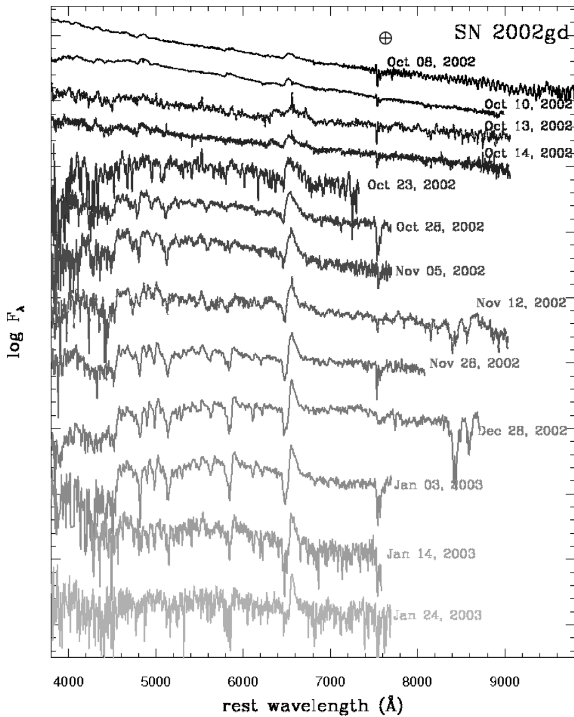**Figure 11.** Spectra of SN 1999gn (top) and SN 2004eg (centre and bottom).

Figure 12. Sequence of spectra of SN 2002gd during the photospheric phase. Symbol $\oplus$ indicates telluric absorptions.

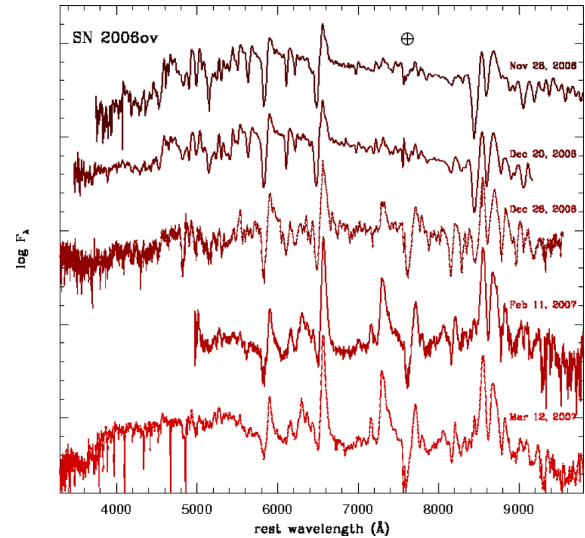**Figure 13.** Spectral evolution of SN 2003Z. Symbol $\oplus$ indicates telluric absorptions.

Figure 14. Sequence of spectra of SN 2006ov from photospheric to nebular phase. Significant contamination from the background explains the blue excess at late phase. Symbol $\oplus$ indicates telluric absorptions.

very blue, becomes rapidly redder ($T \approx 10000$ K at phase 10 d and $T \approx 6000$–8000 K at phase 30 d). The evolution of all the objects of the sample is remarkably homogenous and similar to those of SN 2004et.

Phase ~30–120 d. With cooling, the absorption lines become deeper and shift to redder wavelengths. During the plateau phase, between days ~30 and ~120, narrow metal lines appear, viz. Ba II, Sc II, Fe II, Sr II, Cr II and Ti II (with many multiplets visible below 5400 Å). With time the absorption line components become narrower and more prominent, and Ba II lines become among the strongest features in the SN spectrum.

After the fast drop observed during the earliest period, the expansion velocity settles on to a more gentle decline, with v(Sc II) slowing from 2000 to 1000 km s^{-1} between day 30 and ~120. A similar behaviour is observed also in the temperature evolution (Fig. 15), with temperatures remaining almost constant around 5500–6500 K up to ~120 d. This temperature is close to the recombination temperature for the hydrogen as the photosphere recedes through the envelope.

Phase $\gtrsim$120 d. The end of the recombination phase corresponds to a further decline in the continuum temperature, which settles at $T \sim 4000$–5000 K as the SN enters its nebular phase.

Figure 15. Sc II 6246 Å velocities and continuum temperature evolution of LL SNe IIP.

Table 12. Expansion velocities as derived from the position of the minimum of Hα and the Sc II 6246 Å line, and continuum temperatures.

Phase	v(Hα) km s^{-1}	v(Sc II) km s^{-1}	T_{cont} (K)
		SN 1999gn	
45.7	2130 (120)	1690 (100)	7500 (500)
		SN 2002gd	
3.5	5290 (250)	–	14 500 (300)
5.7	5140 (180)	–	12 700 (400)
9.1	5010 (330)	–	9700 (600)
10.0	4920 (250)	–	9400 (400)
19.0	4680 (340)	–	8500 (800)
24.4	4480 (170)	–	8300 (600)
32.3	4160 (200)	2540 (200)	8100 (800)
38.8	3990 (170)	2110 (360)	7300 (700)
55.5	3580 (170)	1840 (80)	6500 (500)
85.3	2840 (350)	1300 (70)	6100 (400)
91.3	2680 (320)	1250 (90)	6000 (700)
102.3	2530 (450)	1180 (130)	5900 (800)
112.3	2370 (500)	1040 (290)	6000 (600)
		SN 2003Z	
27.5	4380 (260)	2250 (60)	7200 (250)
29.5	4260 (230)	2170 (120)	7200 (450)
37.6	3980 (300)	1890 (120)	6700 (350)
39.5	3900 (300)	1820 (160)	6700 (350)
73.4	1660 (100)	1420 (60)	6100 (300)
74.6	1520 (70)	1350 (70)	6100 (500)
96.5	1130 (60)	1040 (60)	6000 (500)
103.5	1070 (100)	1050 (120)	5800 (600)
153.4	810 (100)	740 (200)	4300 (700)
		SN 2004eg	
93.0	1220 (70)	1160 (240)	6200 (600)
171.6	1440 (410)	1060 (300)	5100 (900)
		SN 2006ov	
93.7	3320 (470)	1310 (100)	6600 (400)
115.7	2980 (580)	1090 (160)	5800 (600)
121.7	2800 (600)	1030 (400)	5300 (700)
168.7	1920 (430)	1010 (700)	5200 (1000)
197.7	1764 (660)	1020 (560)	5100 (700)

The transition to the nebular phase (well visualized by the spectral sequence of SN 2006ov) is characterized by the progressive fading in the strength of permitted metal lines and by the appearance of forbidden emissions: [O I] 6300, 6364 Å, [Fe II] 7155 Å, [Ca II] 7291, 7324 Å. The nebular spectra are very similar to those observed in normal Type IIP: the same forbidden lines are visible but with narrower profiles.

The expansion velocities of the ejecta after 4–5 months, as measured from the FWHM of the strongest lines, are below 1000 km s^{-1}, still a factor of 2–3 times lower than those of normal SNe IIP, and they remain roughly constant during the subsequent months.

6 SYSTEMATICS

CC SNe show a wide variety of properties depending on the configuration of their progenitor stars at the explosion. Even within the subclass of H-rich SNe (IIP) the observed parameters cover a wide range of values. Hamuy (2003) found that the physical parameters of SNe IIP, in particular the average plateau luminosity, the expansion velocity measured at the recombination, the ejected ^{56}Ni mass, the total mass of the ejecta and the kinetic energy, are well correlated. However, the analysis of Hamuy (2003) was biased towards bright objects, and LL SNe IIP were undersampled. Based on only five objects, Pastorello et al. (2004) indicated that LL SNe IIP are not an independent class of core collapse SNe but rather the low velocity, low ^{56}Ni mass, low-energy tail in the distribution of SNe IIP. Here we want to verify this issue on a much larger sample.

During the nebular phase, the SN luminosity is powered by radioactive decay chain ^{56}Ni $\rightarrow$ ^{56}Co $\rightarrow$ ^{56}Fe, and its subsequent deposition of γ-rays and positrons. The ejecta is still opaque to γ-rays therefore the bolometric luminosity at late phases can be considered a good indicator of the amount of ^{56}Ni mass ejected in the explosion. Since typically only optical band observations are available, the pseudo-bolometric light curve obtained integrating the fluxes over several passbands (*BVRI*) can be used as a first approximation to estimate the ^{56}Ni mass. Comparing the late-time pseudo-bolometric luminosities of our SN sample with those of SN 1987A in the same bands and at the same epochs, we can estimate the ^{56}Ni mass ejected by our sample of LL SNe IIP via the relation

$$M_{\mathrm{SN}}(\mathrm{Ni}) = 0.075 \times \frac{L_{\mathrm{SN}}}{L_{87A}} \mathrm{M}_\odot. \qquad (3)$$

A summary of the ^{56}Ni masses as derived from the above relation is reported in Table 13, along with other observables for our SN sample. In the case of SN 2002gd only upper detection limits are available and therefore only an upper limit on the ejected ^{56}Ni mass is calculated. Moreover, in the case of SN 2005cs we noticed that the ratio optical/infrared fluxes in the nebular stages is significantly different from that of SN 1987A (this means that considering the *BVRI* luminosity contribution only does not give a good tool to evaluate the Ni mass of SN 2005cs). For this reason, in the case of SN 2005cs, we derived the nickel mass by comparing the quasi-bolometric (*UVOIR*) luminosities instead of the *BVRI* luminosities.

We investigate the correlation between the absolute magnitude of the plateau in the *V* band and the ejected ^{56}Ni mass derived by Hamuy (2003, see Fig. 16), considering the entire sample of LL SNe IIP (green squares) and an extensive sample of normal to luminous SNe IIP (black squares), the SN sample presented by Hamuy (2003), plus the normal Type IIP SNe 2003gd (Hendry et al. 2005), 2004A (Hendry et al. 2006) and 2004et (Maguire et al. 2010). We plot with red squares SN 2004et as representative of a

2888 S. Spiro et al.

Table 13. Properties of the whole sample of LL SNe IIP. M_V is the mean magnitude in the plateau phase, M_{Ni} is the ejected nickel mass and v_{50} is the velocity at $\sim$50 d after the explosion. Properties of the normal IIP SN 2004et are reported for comparison. References: (1) Pastorello et al. (2004); (2) Turatto et al. (1998); (3) Benetti et al. (2001); (4) this paper; (5) Pastorello et al. (2006); (6) Pastorello et al. (2009); (7) Mattila et al. (2008); (8) Van Dyk et al. (2012); (9) Roy et al. (2011); (10) Takáts et al. (2014); (11) Fraser et al. (2011); (12) Gal-Yam et al. (2011) and (13) Maguire et al. (2010).

SN	t_0 (240 0000+)	μ	A_v	M_V	M_{Ni}	v_{50}	Ref.
1994N	49451 ± 10	33.09 ± 0.31	0.108	-14.68 ± 0.31	0.005 ± 0.001	2110 ± 280	1, 4
1997D	50361 ± 15	30.74 ± 0.92	0.058	-13.97 ± 0.92	0.005 ± 0.004	1910 ± 260	2, 3, 4
1999br	51278 ± 3	30.97 ± 0.83	0.065	-13.42 ± 0.83	0.002 ± 0.001	1640 ± 130	1
1999eu	51394 ± 15	30.85 ± 0.87	0.073	-13.61 ± 0.87	0.001 ± 0.001	1320 ± 110	1, 4
2001dc	51047 ± 5	32.64 ± 0.38	1.250	-14.11 ± 0.40	0.005 ± 0.002	1310 ± 250	1
2002gd	52552 ± 2	32.87 ± 0.35	0.184	-15.49 ± 0.35	<0.003	1840 ± 80	4
2003Z	52665 ± 4	31.70 ± 0.60	0.106	-14.28 ± 0.61	0.005 ± 0.003	1630 ± 190	4
2004eg	53170 ± 30	32.64 ± 0.38	1.237	-14.72 ± 0.40	0.007 ± 0.003	1730 ± 100	4
2005cs	53549 ± 1	29.46 ± 0.60	0.155	-14.86 ± 0.60	0.006 ± 0.003	1715 ± 180	5, 6
2006ov	53974 ± 6	30.5 ± 0.95	0.061	-14.83 ± 0.95	0.002 ± 0.002	1860 ± 200	4
2008bk	54550 ± 1	27.68 ± 0.13	0.065	-14.80 ± 0.13	0.007 ± 0.001	$-$	7, 8
2008in	54825 ± 1	30.60 ± 0.20	0.305	-15.37 ± 0.23	0.012 ± 0.005	2480 ± 170	9
2009N	54848 ± 1	31.67 ± 0.11	0.350	-15.59 ± 0.12	0.020 ± 0.004	1790 ± 280	10
2009md	55162 ± 8	31.64 ± 0.21	0.310	-14.68 ± 0.24	0.004 ± 0.001	2350 ± 130	11
2010id	55452 ± 2	32.86 ± 0.50	0.167	-13.99 ± 0.51	$-$	2040 ± 180	12
2004et	53270 ± 1	28.85 ± 0.34	1.271	-17.15 ± 0.27	0.056 ± 0.040	3990 ± 270	4, 13

Figure 16. Absolute *V*-band magnitude (computed at day 50) versus mass of ^{56}Ni. Green squares represent our LL SN IIP sample, black squares are canonical SNe IIP from Hamuy (2003), Hendry et al. (2005, 2006) and Maguire et al. (2010), red squares are SN 2004et, SN 2005cs and SN 2008in (Roy et al. 2011). When no other distance determinations are available, we computed a kinematic distance using the host galaxy radial velocity corrected for the Local Group infall into Virgo (V_{vir} as reported in the HYPERLEDA data base, with Hubble constant $H_0 = 72$ km s^{-1} Mpc $^{-1}$). The adopted uncertainty in the kinematic distances is computed from the local cosmic thermal velocity 187 km s^{-1}, as in Smartt et al. (2009). For SN 2004et, we adopted $t_0 = 2453270$, $A_v = 1.271$, $\mu = 28.85 \pm 0.34$ (see Table 13).

normal SNe IIP, SN 2005cs as representative of LL SNe IIP and SN 2008in (Roy et al. 2011) as an intermediate case (see Section 7). LL SNe IIP appear to fill the observational gap between the ultrafaint SN 1999br (Pastorello et al. 2004) and the normal Type IIP events. In spite of a large dispersion, LL SNe IIP do not lie in a separate area of the diagram and, confirming the result of Hamuy (2003), we observe a continuum distribution in the ejected ^{56}Ni mass with the SN luminosity in our enlarged sample. Using a weighted
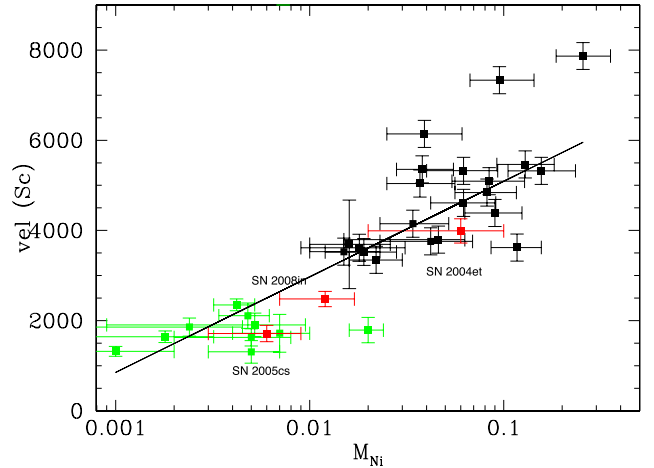

Figure 17. Ejecta velocities versus ^{56}Ni masses. The expansion velocities are obtained from measuring the position of the minimum of the Sc II 6246 Å line. Symbols are as in Fig. 16.

least-squares method, we estimate a correlation coefficient of -0.72 and -0.92 for the normal and entire sample, respectively. In other words, there is clear evidence that SNe with brighter plateaus produce more ^{56}Ni.

In Fig. 17 we tested the correlation between the photospheric expansion velocities, measured from the position of the minimum of the Sc II $\lambda6246$ line at $\sim$50 d after the explosion, and the ejected ^{56}Ni mass, extending the original sample of Hamuy to the new faint objects. Again, LL SNe IIP are labelled with green colours and normal-to-luminous SNe IIP with black colours. It is clear that SNe with larger expansion velocities are those producing more ^{56}Ni, confirming once again the results of Hamuy (2003). Using a weighted least-squares method, we estimate a correlation coefficient of 0.65 and 0.86 for the normal and entire sample, respectively.

From Figs 16 and 17, we confirm that there exists a continuum in the properties of SNe Type II from LL, low velocity and Ni- poor

events such as SN 1997D and SN 1999br, to high luminosity and high velocity SNe IIP (such as SN 1992am; Hamuy 2003).

7 DISCUSSION

Theory predicts that stars with ZAMS masses between $\sim$8–9 $M_\odot$ and $\sim$25–30 $M_\odot$ end their lives as SNe IIP (e.g. Heger et al. 2003). The lower limit for this main-sequence mass range is set by the heaviest stars that are expected to produce a white dwarf whilst the upper limit depends on the details of the pre-SN evolution and the explosion mechanism, and is deeply related to still uncertain parameters such as overshooting, mixing and mass-loss rate (see e.g. Woosley, Heger & Weaver 2002).

Three different possible configurations for the progenitors have been proposed to explain the energetics and the overall properties of LL SNe IIP: (i) a red supergiant star of about $\sim$12 $M_\odot$ which terminates its life when it exhausts the nuclear fuel and its iron core is no longer sustained against gravitational collapse; (ii) an explosion of a more massive ($M \gtrsim 25$ $M_\odot$) star in which a considerable fraction of the material ejected in the explosion falls back into the compact remnant (this event is sometimes labelled as *fall-back SN*); (iii) stars in the mass range $\sim$8–11 $M_\odot$ that forms a degenerate NeO core during the final stage of its evolution and explodes as an electron-capture SN.

In the last decade major efforts have been devoted to constrain the mass of the progenitors of LL SNe IIP. Those were based on two different approaches, i.e. by comparing observations (light curves, colours, spectra) with hydrodynamical models and by direct detection of the progenitor stars in pre-SN images. With the latter approach, after measuring the brightness and colour of the star, the mass can be computed through a comparison with stellar evolution models (see Smartt 2009 for a review). The mass estimates through the two different approaches have been shown to provide somewhat discrepant results with hydrodynamical modelling providing often higher masses for the precursor of SNe IIP.

In this section we aim to derive the physical parameters of two representative objects by hydrodynamical modelling of the SN data: SN 2005cs (which has excellent observational coverage and one can consider it a template for LL SNe IIP) and SN 2008in (an intermediate object between normal and faint SNe IIP). This work is the starting point for a detailed analysis through the modelling of the physical parameters of our full sample of LL SNe II-P that will be presented in a forthcoming paper (Pumo et al., in preparation).

We estimate the main physical properties of the progenitors at the explosion (i.e. the ejected mass, the progenitor radius and the explosion energy) through the hydrodynamical modelling of their main observables (i.e. bolometric light curve, evolution of line velocities and continuum temperature at the photosphere), using the same well-tested approach used for other observed CC SNe (e.g. SNe 2007od, 2009bw, 2009E and 2012A; see Inserra et al. 2011, 2012; Pastorello et al. 2012; Tomasella et al. 2013).

According to this approach, a simultaneous χ^2 fit of the aforementioned observables against model calculations is performed with two codes: a semi-analytic code (Zampieri et al. 2003) which solves the energy balance equation for a homologously expanding envelope of constant density and the general-relativistic, radiation-hydrodynamics Lagrangian code presented in Pumo, Zampieri & Turatto (2010) and Pumo & Zampieri (2011). The latter is able to simulate the evolution of the physical properties of the CC-SN ejecta and the behaviour of the main observables from the breakout of the shock wave at the stellar surface up to the nebular stage. The

distinctive features of this new code are: (a) an accurate treatment of radiative transfer coupled with relativistic hydrodynamics, (b) a fully implicit Lagrangian approach to the solution of the coupled non-linear finite difference system of relativistic radiation-hydro equations and (c) a description of the evolution of ejected material which takes into account both the gravitational effects of the compact remnant and the heating effects linked to the decays of the radioactive isotopes synthesized during the CC-SN explosion.

The semi-analytic code is used to carry out a preparatory study aimed at determining the parameter space describing the CC-SN progenitor at the explosion and, consequently, to guide the more realistic, but time consuming simulations performed with the general-relativistic, radiation-hydrodynamics code.

The approach of modelling with the two codes is appropriate, since the emission of SNe 2005cs and 2008in is dominated by the expanding ejecta. In performing the χ^2 fit, we have neglected the observations obtained before the full relaxation of the plateau ($t < 20$ d) when the observables are significantly affected by emission from the outermost shell of the ejecta (see Pumo & Zampieri 2011 for details). After shock passage, this shell, that contains only a small fraction of the envelope mass (few tenths of solar masses), is accelerated to very high velocities and is not in homologous expansion. The structure, evolution and emission properties of this shell are not well reproduced in our simulations because at present we adopt an 'ad hoc' initial density profile, not derived from an explosion simulation coupled with pre-SN evolutionary models.

The best-fitting models for SNe 2005cs and 2008in are shown in Figs 18 and 19, respectively.

For SN 2005cs, assuming a ^{56}Ni mass of $\sim$0.0065 $M_\odot$, an explosion epoch JD = 245 3549 and a distance modulus of 29.46 ± 0.60 mag (see Table 13), the best fit returns values of total (kinetic plus thermal) energy of $E = 0.16$ foe, initial radius of $R = 2.5 \times 10^{13}$ cm and envelope mass of $M_{env} = 9.5$ $M_\odot$, in good agreement with the parameters obtained from our previous modelling reported in Pastorello et al. (2009). The estimated uncertainty on the best-fitting model parameters E, M_{env} and R is
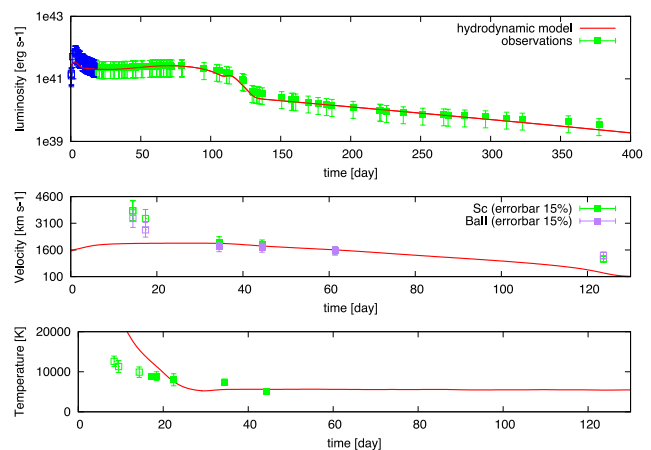

Figure 18. Comparison of the evolution of the main observables of SN 2005cs with the best-fitting model computed the general-relativistic, radiation-hydrodynamics code (total energy 0.16 foe, initial radius 2.5 × 10^{13} cm, envelope mass 9.5 $M_\odot$). Top, middle and bottom panels show the bolometric light curve, the photospheric velocity, and the photospheric temperature as a function of time. Blue symbols in the top panel and open symbols in the middle and bottom panels mark early observations (<20 d) not considered in the fit (see the text for details). Photospheric velocities are those derived from the minima of the P Cygni profiles of the Sc II and Ba II lines.
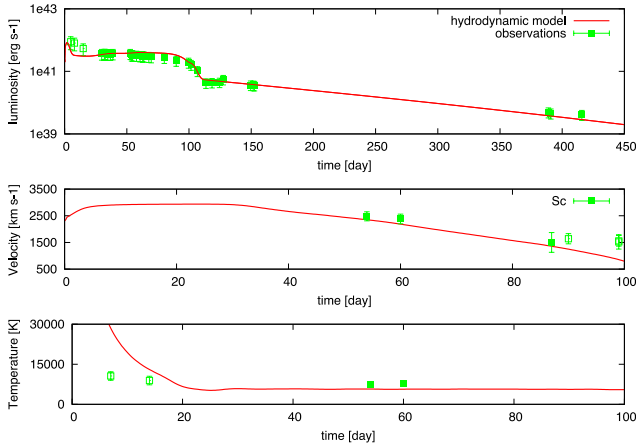
Figure 19. Comparison of the evolution of the main observables of SN 2008in with the best-fitting model computed with the general-relativistic, radiation-hydrodynamics code (total energy 0.49 foe, initial radius 1.5 × 10^{13} cm, envelope mass 13 M$_\odot$). The three panels are similar to those of Fig. 18.

$\lesssim$20 per cent. The values reported above are consistent with the explosion of a moderate-mass star. Indeed, adding the mass of the compact remnant (∼1.5 M$_\odot$) to that of the ejected material, we obtain that the mass of the progenitor of SN 2005cs at the explosion was ∼11 M$_\odot$. Since the observables of all other LL SNe of our sample are rather similar to those of SN 2005cs, it is reasonable to assume that they share similar physical parameters as those inferred for SN 2005cs (a detailed analysis will be reported in Pumo et al., in preparation).

The situation is different for SN 2008in (Roy et al. 2011) whose observed parameters are intermediate between those of canonical SNe IIP and LL SNe IIP. As for SN 2005cs, adopting a ^{56}Ni mass of ∼0.012 M$_\odot$, an explosion epoch JD = 245 4825.6 and a distance modulus of 30.60 ± 0.20 mag (see Table 13), the best-fitting model returns values of total (kinetic plus thermal) energy of E = 0.49 foe, initial radius of R = 1.5 × 10^{13} cm, and envelope mass of $M_{\rm env}$ = 13 M$_\odot$. Again, the estimated uncertainty on the best-fitting model parameters E, $M_{\rm env}$ and R is $\lesssim$20 per cent. These values are consistent with the explosion of an intermediate-mass star, slightly more massive than the progenitor of SN 2005cs. Adding the mass of the compact remnant to that of the ejected material, we obtain that the mass of the progenitor of SN 2008in at the explosion was of ∼14.5 M$_\odot$.

Up to now, a relatively small number of LL SNe IIP have been discovered. This is plausibly due to selection effects due to their faint intrinsic luminosity rather than intrinsic rarity. Among this restricted sample, hydrodynamical models were compared with observables of five objects (SN 1997D, SN 1999br, SN 2003Z, SN 2005cs and SN 2008in).

Zampieri et al. (2003) found a relatively massive progenitor (19 M$_\odot$) for SN 1997D (revised downwards to 14 ± 2 M$_\odot$ in Zampieri 2007). The low amount of ^{56}Ni observed was explained as due to fall back of material on to the collapsed remnant. An intermediate mass of 16 M$_\odot$ for the progenitor was found by Zampieri et al. (2003) for SN 1999br (revised to 10 ± 1.5 M$_\odot$ in Zampieri 2007) and of 15.9 ± 1.5 M$_\odot$ for SN 2003Z by Utrobin et al. (2007). In the case of SN 2005cs, the best observed LL SNe IIP, several groups reported hydrodynamic masses of 18.2 ± 1 M$_\odot$ (Utrobin & Chugai 2008), 10–15 M$_\odot$ (Pastorello et al. 2009) to be compared with the new value of ∼11 M$_\odot$ obtained here with the new hy-

drodynamical model. Finally, we find the mass of the progenitor of SN 2008in at the explosion to be ∼ 14.3 M$_\odot$, in good agreement with Utrobin & Chugai (2013) who found a progenitor mass of 15.5 ± 2.2 M$_\odot$ (including the mass-loss effects) for the same object. The differences among the results obtained with different hydrodynamical approaches, are likely a consequence of different assumptions about the input physics (in particular the opacity) and of different choices of distance moduli or total extinction [e.g. μ = 29.62 versus μ = 29.26 and $E(B - V)$ = 0.12 mag versus $E(B - V)$ = 0.05 mag assumed by Utrobin & Chugai (2008) and Pastorello et al. (2009), respectively, for SN 2005cs]. Despite these differences, recent results from hydrodynamical modelling now converge to low–intermediate masses for LL SNe IIP.

Hydrodynamical models have been applied also to well-studied normal SNe IIP, e.g. SN 1999em and SN 2004et. In the case of SN 1999em a pre-SN radius of R ∼ (3.5−6.9) × 10^{13} cm, an ejecta mass of 18–19 M$_\odot$, an explosion energy of 1–1.3 foe and a radioactive ^{56}Ni mass of 0.036–0.06 M$_\odot$ were estimated (Utrobin 2007b; Baklanov, Blinnikov & Pavlyuk 2005; Bersten, Benvenuto & Hamuy 2011). Larger values for the physical parameters were obtained in the case of SN 2004et: R ∼ 10^{14} cm, $M_{\rm env}$ = 24.5 M$_\odot$, E ∼ 2.3 foe, $M_{\rm Ni}$ ∼ 0.068 M$_\odot$ (Utrobin & Chugai 2009).

Despite the fact that the values reported above were derived by different hydrodynamical codes with different assumption, physics, etc. we speculate that there could be a general trend in the parameters of SNe IIP, as claimed by Hamuy (2003). Less energetic explosions preferentially produce less luminous events and lower mass of ^{56}Ni. Moreover, the parameters inferred from data modelling of LL SNe IIP appear now to agree with the analysis of pre-SN images in suggesting that stars of relatively low-to-intermediate mass produce LL SNe while normal SNe IIP derive from progenitors of larger mass. A more sophisticated hydrodynamical modelling of LL SNe IIP is in progress (Pumo et al., in preparation) to strengthen this speculation.

8 SUMMARY

In this paper we have presented new data for five LL SNe IIP and investigated their observational properties, comparing them with a comprehensive sample of objects. We have shown that all LL SNe IIP have very homogeneous photometric and spectroscopic evolutions. In particular they display surprisingly consistent colour evolutions, expansion velocities of the ejected material and amounts of ^{56}Ni synthesized (see Table 13). We have investigated the correlations of the ejected ^{56}Ni masses with the plateau magnitudes and expansion velocities of the ejecta, and showed that these faint events are the LL tail of a continuous distribution of otherwise normal explosions, instead of a separate class of CC SNe. Finally we have discussed the preliminary results of a systematic hydrodynamical modelling of the observables of LL SNe IIP that will be presented more extensively in a forthcoming paper. The hydrodynamical masses estimates for SN 2005cs and for SN 2008in suggest that LL SNe IIP originate from low-to-intermediate mass stars in the range 10–15 M$_\odot$, in good agreement with the mass trend suggested by the direct progenitor detection method (Smartt et al. 2009).

It seems that results from our modelling and direct detection of the progenitor in pre-explosion images are converging towards a low-to-intermediate mass scenario (see also Tomasella et al. 2013). Indeed the results presented in this paper for SN 2005cs and SN 2008in reduce the gap between progenitor masses estimated through hydrodynamical modelling or direct detection in pre-SN archive

images, pointing to red supergiants of moderate mass or, less commonly, to super asymptotic giant branch (AGB) stars (although the possibility to have electron-capture SN from super-AGB progenitor is strongly questioned; e.g. Eldridge et al. 2007). Differences in the light curves or in the spectral properties among the events reported here could be trivially explained with slightly different values of energies, radii or ejected masses.

REFERENCES

Ayani K., Yamaoka H., 1999, IAU Circ., 7336, 1
Baklanov P. V., Blinnikov S. I., Pavlyuk N. N., 2005, Astron. Lett., 31, 429
Benetti S. et al., 2001, MNRAS, 322, 361
Benetti S., Altavilla G., Pastorello A., Riello M., Turatto M., Zampieri L., Cappellaro E., Germany L., 2002, IAU Circ., 7987, 3
Berger E. et al., 2009, ApJ, 699, 1850
Bersten M. C., Benvenuto O., Hamuy M., 2011, ApJ, 729, 61
Blondin S., Modjaz M., Kirshner R., Challis P., Berlind P., 2006, Cent. Bureau Electron. Telegrams, 757, 1
Boles T., Beutler B., Li W., Qiu Y. L., Hu J. Y., Schwartz M., 2003, IAU Circ., 8062, 1
Bond H. E., Bedin L. R., Bonanos A. Z., Humphreys R. M., Monard L. A. G. B., Prieto J. L., Walter F. M., 2009, ApJ, 695, L154
Botticella M. T. et al., 2009, MNRAS, 398, 1041
Brown P. J. et al., 2007, ApJ, 659, 1488
Chugai N. N., Utrobin V. P., 2000, A&A, 354, 557
Crockett R. M., Smartt S. J., Pastorello A., Eldridge J. J., Stephens A. W., Maund J. R., Mattila S., 2011, MNRAS, 410, 2767
de Mello D., Benetti S., Massone G., 1997, IAU Circ., 6537, 1
Dessart L. et al., 2008, ApJ, 675, 644
Dessart L., Hillier D. J., Waldman R., Livne E., 2013, MNRAS, 433, 1745
Dimai A., Li W., 1999, IAU Circ., 7335, 1
Eldridge J. J., Mattila S., Smartt S. J., 2007, MNRAS, 376, L52
Filippenko A. V., Chornock R., 2002, IAU Circ., 7987, 4
Filippenko A. V., Ganeshalingam M., Serduke F. J. D., Hoffman J. L., 2004, IAU Circ., 8404, 1
Foley R. J. et al., 2009, AJ, 138, 376
Fraser M. et al., 2011, MNRAS, 417, 1417
Gal-Yam A. et al., 2011, ApJ, 736, 159
Garcia A. M., 1993, A&AS, 100, 47
Hamuy M., 2002, IAU Circ., 7987, 2
Hamuy M., 2003, ApJ, 582, 905
Harutyunyan A. H. et al., 2008, A&A, 488, 383
Heger A., Fryer C. L., Woosley S. E., Langer N., Hartmann D. H., 2003, ApJ, 591, 288
Hendry M. A. et al., 2005, MNRAS, 359, 906
Hendry M. A. et al., 2006, MNRAS, 369, 1303
Inserra C. et al., 2011, MNRAS, 417, 261
Inserra C. et al., 2012, MNRAS, 422, 1122
Jerkstrand A., Fransson C., Maguire K., Smartt S., Ergon M., Spyromilio J., 2012, A&A, 546, A28
Klotz A., Jasinski C., 2002, IAU Circ., 7990, 4
Klotz A., Puckett T., Langoussis A., Wood-Vasey W. M., Aldering G., Nugent P., Stephens R., 2002, IAU Circ., 7986, 1
Knop S., Hauschildt P. H., Baron E., Dreizler S., 2007, A&A, 469, 1077
Kochanek C. S., Khan R., Dai X., 2012, ApJ, 759, 20
Kulkarni S. R. et al., 2007, Nature, 447, 458
Li W., Van Dyk S. D., Filippenko A. V., Cuillandre J.-C., Jha S., Bloom J. S., Riess A. G., Livio M., 2006, ApJ, 641, 1060
Li W., Wang X., Van Dyk S. D., Cuillandre J.-C., Foley R. J., Filippenko A. V., 2007, ApJ, 661, 1013
Maguire K. et al., 2010, MNRAS, 404, 981
Maguire K. et al., 2012, MNRAS, 420, 3451
Matheson T., Challis P., Kirshner R., Calkins M., 2003, IAU Circ., 8063, 2
Mattila S., Smartt S. J., Eldridge J. J., Maund J. R., Crockett R. M., Danziger I. J., 2008, ApJ, 688, L91
Maund J. R., Smartt S. J., 2005, MNRAS, 360, 288
Maund J. R., Smartt S. J., Danziger I. J., 2005, MNRAS, 364, L33
Maund J. R., Mattila S., Ramirez-Ruiz E., Eldridge J. J., 2014, MNRAS, 438, 1577
Maund J. R., Reilly E., Mattila S., 2014, MNRAS, 438, 938
Nakano S., Itagaki K., Kadota K., 2006, Cent. Bureau Electron. Telegrams, 756, 1
Nomoto K., 1984, ApJ, 277, 791
Pastorello A. et al., 2004, MNRAS, 347, 74
Pastorello A. et al., 2006, MNRAS, 370, 1752
Pastorello A. et al., 2007, Nature, 449, E1
Pastorello A. et al., 2009, MNRAS, 394, 2266
Pastorello A. et al., 2012, A&A, 537, A141

Paturel G., Petit C., Prugniel Ph., Theureau G., Rousseau J., Brouty M., Dubois P., Cambrésy L., 2003, A&A, 412, 45

Pumo M. L., 2007, Mem. Soc. Astron. Ital., 78, 689

Pumo M. L., Zampieri L., 2011, ApJ, 741, 41

Pumo M. L. et al., 2009, ApJ, 705, L138

Pumo M. L., Zampieri L., Turatto M., 2010, Mem. Soc. Astron. Ital. Suppl., 14, 123

Rau A. et al., 2009, PASP, 121, 1334

Roy R. et al., 2011, ApJ, 736, 76

Schlafly E. F., Finkbeiner D. P., 2011, ApJ, 737, 103

Skrutskie M. F. et al., 2006, AJ, 131, 1163

Smartt S. J., 2009, ARA&A, 47, 63

Smartt S. J., Maund J. R., Hendry M. A., Tout C. A., Gilmore G. F., Mattila S., Benn C. R., 2004, Science, 303, 499

Smartt S. J., Eldridge J. J., Crockett R. M., Maund J. R., 2009, MNRAS, 395, 1409

Smith J. A. et al., 2002, AJ, 123, 2121

Smith N. et al., 2009, ApJ, 697, L49

Takahashi K., Yoshida T., Umeda H., 2013, ApJ, 771, 28

Takáts K., Vinkó J., 2006, MNRAS, 372, 1735

Takáts K. et al., 2014, MNRAS, 438, 368

Tomasella L. et al., 2013, MNRAS, 434, 1636

Tsvetkov D. Y., Volnova A. A., Shulga A. P., Korotkiy S. A., Elmhamdi A., Danziger I. J., Ereshko M. V., 2006, A&A, 460, 769

Turatto M. et al., 1998, ApJ, 498, L129

Utrobin V. P., 2007, A&A, 461, 233

Utrobin V. P., Chugai N. N., 2008, A&A, 491, 507

Utrobin V. P., Chugai N. N., 2009, A&A, 506, 829

Utrobin V. P., Chugai N. N., 2013, A&A, 555, 145

Utrobin V. P., Chugai N. N., Pastorello A., 2007, A&A, 475, 973

Valenti S. et al., 2009, Nature, 459, 674

Van Dyk S. D., Li W., Filippenko A. V., 2003, PASP, 115, 21

Van Dyk S. D. et al., 2012, AJ, 143, 19

Walmswell J. J., Eldridge J. J., 2012, MNRAS, 419, 2054

Woosley S. E., Heger A., Weaver T. A., 2002, Rev. Mod. Phys., 74, 1015

Yoshii Y., 2002, in Sato K., Shiromizu T., eds, Proc. RESCEU Int. Symp. 5, New Trends in Theoretical and Observational Cosmology. Universal Academy Press, Tokyo, p. 235

Yoshii Y., Kobayashi Y., Minezaki T., 2003, Am. Astron. Soc., 35, 752

Young J., Boles T., Li W., 2004, IAU Circ., 8401, 2

Zampieri L., 2007, in Antonelli L. A., Israel G. L., Piersanti L., Tornambe A., Burderi L., Di Salvo T., Fiore F., Matt G., Menna M. T., eds, AIP Conf. Proc. Vol. 924, The Multicolored Landscape of Compact Objects and their Explosive Origins. Am. Inst. Phys., New York, p. 358

Zampieri L., Shapiro S. L., Colpi M., 1998, ApJ, 502, L149

Zampieri L., Pastorello A., Turatto M., Cappellaro E., Benetti S., Altavilla G., Mazzali P., Hamuy M., 2003, MNRAS, 338, 711

This paper has been typeset from a TEX/LATEX file prepared by the author.